

# UNCLASSIFIED

AD NUMBER
AD251478
NEW LIMITATION CHANGE
TO Approved for public release, distribution unlimited
FROM Distribution authorized to U.S. Gov't. agencies and their contractors; Administrative/Operational Use; SEP 1960. Other requests shall be referred to Air Force Special Weapons Center, Kirtland AFB, NM.
AUTHORITY
AFWL ltr, 25 May 1970

THIS PAGE IS UNCLASSIFIED

**UNCLASSIFIED**

---

**AD 251 478**

---

*Reproduced  
by the*

**ARMED SERVICES TECHNICAL INFORMATION AGENCY  
ARLINGTON HALL STATION  
ARLINGTON 12, VIRGINIA**



---

**UNCLASSIFIED**

NOTICE: When government or other drawings, specifications or other data are used for any purpose other than in connection with a definitely related government procurement operation, the U. S. Government thereby incurs no responsibility, nor any obligation whatsoever; and the fact that the Government may have formulated, furnished, or in any way supplied the said drawings, specifications, or other data is not to be regarded by implication or otherwise as in any manner licensing the holder or any other person or corporation, or conveying any rights or permission to manufacture, use or sell any patented invention that may in any way be related thereto.

AFSWC-TN-60-36

SWC  
TN  
60-36

CATALOGED BY ASTIA  
AS AD NO. \_\_\_\_\_

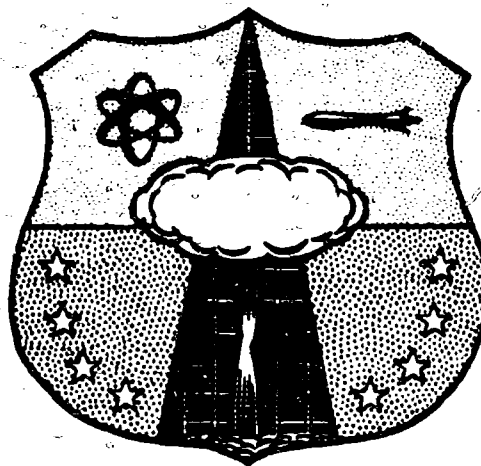
251 478

## HEADQUARTERS

# AIR FORCE SPECIAL WEAPONS CENTER

AIR RESEARCH AND DEVELOPMENT COMMAND

KIRTLAND AIR FORCE BASE, NEW MEXICO



Technical Note

### DESIGN AND ANALYSIS OF FOUNDATIONS FOR PROTECTED STRUCTURES

Interim Technical Report

by

K. E. McKee

Armour Research Foundation of  
Illinois Institute of Technology  
Technology Center  
Chicago 16, Illinois

September 1960

XEROX

AFSWC-TN-60-36

DESIGN AND ANALYSIS OF FOUNDATIONS  
FOR PROTECTIVE STRUCTURES

Interim Technical Report

by

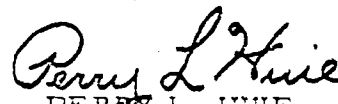
K. E. McKee

Armour Research Foundation of  
Illinois Institute of Technology  
Technology Center  
Chicago 16, Illinois

September 1960

Research Directorate  
AIR FORCE SPECIAL WEAPONS CENTER  
Air Research and Development Command  
Kirtland Air Force Base, New Mexico

Approved:



PERRY L. HUIE  
Colonel USAF  
Chief, Structures Division

Project No. 1080  
Task No. 10803  
Contract No. AF 29(601)-2561  
ARF Project No. K193



LEONARD A. EDDY  
Colonel USAF  
Director, Research Directorate

# ABSTRACT

The behavior of footings subjected to time-dependent forces has been the subject of continuing research. The ultimate bearing capacity under such loading conditions and the dynamic behavior beyond this ultimate capacity are both of interest. An attempt has been made in the subject investigation to combine and correlate laboratory experiments with theoretical studies.

Two- and three-dimensional experiments have been conducted on small footings in the laboratory to observe their behavior and to obtain quantitative information. An apparatus was developed for applying dynamic forces to the footings. This apparatus, which is relatively simple, has made possible the application of loads having various rise times, decays, and durations. Force-time and displacement-time records have been obtained in forms suitable for analysis, and Fastax movies of footings failing under dynamic loads have also been taken.

The behavior of footings subjected to dynamic loads has been studied analytically also. The possibility of applying the plasticity theory or limit analysis has been considered. Other loadings and various failure modes also have been investigated. Use will be made of the experimental data in conjunction with this theoretical work during the remainder of the program. Based on this work, additional experimental and/or theoretical research will be conducted as required.

## PUBLICATION REVIEW

This report has been reviewed and is approved.



CAREY L. O'BRYAN, JR.  
Colonel USAF  
Deputy Commander

## PREFACE

This is the interim technical report on Contract No. AF29(601)-2561, Project 1080, "Design and Analysis of Foundations for Protective Structures". The object of this research program is to investigate the problems associated with the design and analysis of foundations for protective structures which are subjected to dynamic loads from nuclear blast. The current project, which was initiated in February, 1960, to a large extent is a continuation of research done on an earlier contract, AF29(601)-1161, which had the same title.

This interim technical report covers the work done on the project during the seven months following the inception of the contract. In organizing this report, an attempt was made to collect the primary technical results into appendices which subsequently can be incorporated into the final report.

Personnel who have contributed to the work covered in this report includes: R. L. Chiapetta, C. J. Costantino, P. G. Hodge, A. Humphreys, K. E. McKee, R. D. Rowe, R. W. Sauer, E. T. Selig, S. Shankman, and E. Vey. Credit should also be given to Mr. C. Wiehle and Mr. H. Mason of AFSWC for their criticisms and suggestions which have aided this project.

## TABLE OF CONTENTS

ABSTRACT .....	<u>Page</u> iii
PREFACE .....	iv
<u>Chapter</u>	
1 INTRODUCTION.....	1
A. General .....	1
B. Objectives.....	1
C. Technical Approach.....	2
D. Discussion of the Problem.....	2
E. Report Organization.....	3
2 THEORETICAL INVESTIGATION.....	4
A. General.....	4
B. Plasticity Theory in Soil Mechanics.....	4
C. Dynamic Response.....	5
D. Non-Vertical Loads.....	8
3 EXPERIMENTAL INVESTIGATION.....	12
A. General.....	12
B. Material Properties.....	12
C. Two-Dimensional Studies.....	13
D. Three-Dimensional Studies.....	13
4 CONCLUSIONS.....	14



## TABLE OF CONTENTS, cont.

### Appendix

A	APPLICATION OF PLASTICITY AND LIMIT ANALYSIS TO FOOTING DESIGN .....	16
A.1	Introduction.....	17
A.2	Plasticity Theory.....	18
A.3	Limit Theories.....	21
A.4	Previous Studies.....	25
A.5	Illustrative Problem.....	28
A.6	Dynamic Problem.....	32
A.7	References.....	33
B	THE METHOD OF CHARACTERISTICS APPLIED TO PROBLEMS OF PLANE PLASTIC STRAIN WITH INERTIAL EFFECTS.....	35
B.1	Introduction.....	36
B.2	Basic Equations.....	37
B.3	Difference Equations for Small Deformations.....	42
B.4	Example.....	48
B.5	Conclusions.....	51
B.6	References.....	52
C	FOOTINGS SUBJECTED TO ECCENTRIC LOADS.....	58
C.1	Introduction.....	59
C.2	Static Loads.....	60
C.3	Dynamic Loads.....	61
D	PROPERTIES OF OTTAWA SAND.....	66
E	TWO-DIMENSIONAL STUDIES.....	73
E.1	Introduction.....	74
E.2	Static Tests.....	74
E.3	Dynamic Tests.....	75
F	THREE-DIMENSIONAL STUDIES.....	88
F.1	Introduction.....	89
F.2	Static Tests.....	89
F.3	Dynamic Tests.....	90
G	DYNAMIC LOADING APPARATUS.....	92

## LIST OF ILLUSTRATIONS

<u>Figure</u>		<u>Page</u>
1	SIMPLIFIED TWO-SIDED FAILURE MODE BASED ON PRANDTL'S SOLUTION.....	10
2	SIMPLIFIED TWO-SIDED FAILURE MODE BASED ON HILL'S SOLUTION.....	11

## APPENDICES

A.1	AN EQUILIBRIUM SOLUTION.....	34
A.2	A VELOCITY SOLUTION.....	34
B.1	CURVILINEAR COORDINATE SYSTEM.....	55
B.2	TYPICAL MESH IN CHARACTERISTIC NET.....	55
B.3	PUNCH ON HALF-SPACE: DIMENSIONS AND STATIC SOLUTION.....	56
B.4	PUNCH ON HALF-SPACE: NATURE OF SOLUTION AND BOUNDARY CONDITIONS.....	57
C.1	ONE-SIDED FAILURE.....	63
C.2	STATIC LOAD vs. FOOTING WIDTH AS A FUNCTION OF $e$ .....	64
C.3	RADIUS vs. FOOTING WIDTH AS A FUNCTION OF $e$ .....	65
D.1	GRAIN SIZE DISTRIBUTION FOR OTTAWA SAND, BOTH NEW SAND AND ORIGINAL SAND.....	70
D.2	FAILURE ENVELOPES FOR OTTAWA SAND AS DETERMINED FROM DIRECT SHEAR TESTS.....	71
D.3	RESULTS OF TRIAXIAL TESTS ON OTTAWA SAND....	72
E.1	FOOTING TESTS IN GLASS BOX, DENSE SAND, 3-in. WIDE FOOTING.....	77

LIST OF ILLUSTRATIONS, cont.

E.2	FOOTING TESTS IN GLASS BOX, LOOSE SAND, 3-in. WIDE FOOTING.....	78
E.3	STATIC FOOTING FAILURE ON DENSE SAND.....	79
E.3	STATIC FOOTING FAILURE ON DENSE SAND.....	80
E.4	STATIC FOOTING FAILURE ON LOOSE SAND.....	81
E.4	STATIC FOOTING FAILURE ON LOOSE SAND.....	82
E.5	FOOTING BEHAVIOR ON COHESIVE SOIL.....	83
E.6	COHESIVE SOIL IN GLASS BOX BEFORE TEST.....	84
E.7	COHESIVE SOIL IN GLASS BOX DURING STATIC TEST....	84
E.8	COHESIVE SOIL AFTER GLASS IN BOX FAILED.....	84
E.9	DYNAMIC TEST OF FOOTING ON DENSE OTTAWA SAND.....	85
E.9	DYNAMIC TEST OF FOOTING ON DENSE OTTAWA SAND.....	86
E.10	DYNAMIC TEST OF FOOTING ON LOOSE OTTAWA SAND.....	87
F.1	4-in. SQUARE FOOTING AFTER FAILURE.....	91
F.2	3-in. SQUARE FOOTING AFTER FAILURE.....	91
G.1	SKETCH OF DYNAMIC APPARATUS.....	95
G.2	DYNAMIC APPARATUS ON GLASS BOX.....	95
G.3	DYNAMIC APPARATUS ON SAND BOX.....	96
G.4	RECORDS FOR 4-in. x 4-in. FOOTING, TEST NO. 6....	97
G.5	RECORDS FOR 4-in. x 4-in. FOOTING, TEST NO. 2.....	98
G.6	TYPICAL CONSOLIDATED RECORDS, TEST NO. 4 .....	99
G.7	TYPICAL CONSOLIDATED RECORDS, TEST NO. 10.....	100

## Chapter 1

### INTRODUCTION

#### A. General

The purpose of this research program is to consider "the design and analysis of foundation for protective structures subjected to dynamic loads from nuclear blast". Within this general research area, there are almost unlimited technical problems that could be considered. This report is concerned with the work done since the inception of the present program in February, 1960.

In this report, it is assumed that the reader is familiar with the results of the previous research conducted by ARF in the same problem area (Contract AF29(601)-1161).<sup>1</sup> For all practical purposes, the research reported herein represents an extension of the previous program. Despite this close association, it has been the aim to make this report readable without supplementary references.

This report is organized to present a self-contained progress report of the technical work. To the maximum extent possible, detailed technical presentations are confined to the appendices with the body of the report limited to general presentations, conclusions, etc. It is to be expected that the reader will make use of these appendices, and little technical information is reproduced in the main body.

#### B. Objectives

The objective stated in the contract is "to investigate the problems associated with the design and analysis of foundations for protective structures which are subjected to dynamic loads from nuclear blasts". This general objective really indicates little regarding the technical direction of the program. The more specific goals of the present program are limited to consideration of spread footings (this is contrasted to foundations in general). At least from a qualitative point-of-view, it was postulated in the original program that behavior of all foundations could be explained by an understanding of the behavior of spread footings and pile foundations with other foundations

---

<sup>1</sup> McKee, K.E., Design and Analysis of Foundations for Protective Structures  
AFSWC-TR-59-56, 15 Oct. 1959.

being considered as some combination of these two. Attention in this program has been devoted to two main problem areas which have been investigated concurrently: studies of dynamic behavior footings have been concerned primarily with vertical loads where the static behavior is understood relatively well and studies of footing behavior under other than centrally applied vertical loads which to date have been carried out primarily for the static case.

C. Technical Approach

The approach has been a combination of analytical and experimental work. In a virgin technical area, it is desirable that these two research tools proceed together. A highly developed theoretical approach, regardless of its technical sophistication or elegance, must be able to withstand the harsh light of experimental reality. On the other hand, experimentation by itself may furnish a mass of useless data if theoretical work is not available to provide a basis for correlation. A purely empirical approach is always expensive and unless there is a satisfactory understanding of the phenomena, it may lead to misinterpretations.

D. Discussion of the Problem

The behavior of footings subjected to dynamic loads represents a major technical area in which little work has been done. The particular objective of this project is somewhat restrictive since consideration is limited to those aspects related to protective construction. The actual reduction represented by this objective is primarily with respect to application rather than fundamental requirements.

Quantitative information relating to the behavior of small footings subjected to dynamic loads has been obtained under this program for limited soil types. Additional experimental data is currently being obtained. It is anticipated that the analysis of this data will provide a quantitative understanding of footing behavior. As this analysis proceeds the direction for future research should become obvious.

Only one previous experimental study of the behavior of footings subjected to dynamic loads is known to the author. In 1954, Massachusetts Institute

of Technology conducted limited static and dynamic footing tests<sup>1/</sup>. Currently three other agencies are testing footings subjected to dynamic loads: Naval Civil Engineering Laboratory, Port Hueneme, California; University of Illinois, Urbana, Illinois; and Waterways Experiment Station, Vicksburg, Mississippi. For information on these programs the reader is referred to these agencies.

#### E. Report Organization

The main body of this report is primarily descriptive in nature. Chapter 2 considers the theoretical work, while Chapter 3 is concerned with the experimental studies. Chapter 4, Conclusions, attempts to generalize what has been done on this program to date, and indicates the direction the research will follow for the remainder of the project.

The first two appendices deal with plasticity and limit analyses. Appendix A presents a general review of pertinent plasticity studies and a discussion of their advantages and limitations. Appendix B represents a first approach at applying the methods of plasticity to the dynamic behavior of footings. Appendix C extends the earlier theoretical studies to include eccentric loads. Appendix D considers the Ottawa sand used in the experimental program. The next two appendices, E and F, report on the two- and three-dimensional footing tests which have been conducted to date. Finally, Appendix G contains information on the dynamic loading apparatus constructed for this project.

---

<sup>1/</sup> Massachusetts Institute of Technology, The Behavior of Soils Under Dynamic Loading, 3, Final Report on Laboratory Studies, AFSWP 118, Aug 1954.

THEORETICAL INVESTIGATION

A. General

The close association of the theoretical research with the laboratory investigations makes any clear distinction between theory and experimentation nearly impossible and certainly undesirable. This chapter discusses primarily the theoretical work with reference to the laboratory studies as required. The theoretical work has proceeded on several fronts. An attempt will be made to report progress, evaluate the suitability of the approach, and indicate the direction of future studies.

B. Plasticity Theory in Soil Mechanics

The instability of the soil below a footing is associated with the formation of shear surfaces. Many of the approaches used for stability problems by soil mechanics engineers rest on approximate extensions of certain classical plasticity solutions, e.g., Prandtl's solution for footing failure. The soil mechanicians from this basis have proceeded, in general, with an engineering point-of-view using assumed failure surfaces and simplifications to treat stability problems. Occasional forays into soil mechanics have been made by plasticians who have considered methods of solution and have solved specific problems. Neither the soil mechanics nor the plasticity theories provide completely satisfactory solutions -- neither approach is able to accurately predict the behavior of an actual footing.

Attention during the original program<sup>1/</sup> was limited to modifications and extensions of more-or-less standard soil mechanics approaches. Based on the original research, it was thought that the more esoteric plasticity approaches could be justified. The experimental phases of the original program raised serious doubts regarding the suitability of "standard" soil mechanics solutions to the

---

<sup>1/</sup> McKee, K. E., Op. cit.

the prediction of the behavior of footings subjected to dynamic loads. The plasticity approach, although complex for practical applications, gave hope of providing a better understanding of the phenomena involved. Appendices A and B are the result of these plasticity considerations.

Appendix A contains a general discussion of the plasticity and limit analysis theory with particular attention given to the potential application to soil mechanics. A number of papers relating the two subjects are considered to demonstrate previous work in this area. In preparing this appendix, an attempt was made to provide an introduction to the theory of plasticity for those not well versed in this field. Most of this appendix is concerned with static problems, with the concept of dynamic solutions being introduced only in general terms.

Appendix B is specifically concerned with an investigation of a theoretical approach, based on the plasticity theory, to the behavior of a footing subjected to dynamic loads. The purpose of the research was to consider first, if such a solution were possible, and, second, to set up a method of approach. The possibility of a theoretical approach was established under certain restrictive assumptions and an example was presented. Greater generalization to extend the solution to other problems seems to be possible although the actual labor of obtaining such solutions is expected to increase substantially. The over-all results of this appendix are most interesting since the possibility of this type of theoretical approach has been established. From the point-of-view of long-range research into the behavior of footings under dynamic loads, this type of approach may provide the final answer and additional studies in this area should be considered.

#### C. Dynamic Response

The behavior of footings subjected to dynamic loads was analyzed in the original report by what might be termed an "engineering approach". This approach was based on an extension to time-dependent loads of Andersen's<sup>1/</sup>

---

<sup>1/</sup> Andersen, P., Substructure Analysis and Design, The Ronald Press, New York, New York, 1956, p. 87.



work relating to one-sided footing failure. The major assumptions introduced for this approach are:

1. The failure surface under dynamic loads will be the surface determined by application of the initial value of the over-pressure as static pressure.
2. The resistance offered to movement is rigid plastic in form, i.e., settlement and soil compressibility are not considered.
3. The maximum plastic resistance equals the static resistance determined analytically, assuming the failure surfaces considered are the same as in item 1 above.
4. The behavior of the soil is governed by the parameters  $\gamma$ ,  $\phi$ , and  $c$ , where  $\phi$  and  $c$  may themselves be functions of many parameters relating to the soil and the condition of loading.

By considering the motion of the failure mass of soil, a differential equation was established for the dynamic behavior. Solutions of this equation allow prediction of the displacements, investigation of inertia effects, etc.

In the original program, the one-sided failure pattern (Andersen's) was specially selected because it was compatible with the dynamic analysis. This compares with other failure assumptions, such as Terzaghi's modification of Prandtl's solution, for which the failure mode is compatible only for incipient motion. Two-sided failure patterns generally are not suitable for gross motion. Since two-sided failures do occur, an attempt has been made to consider possible two-sided failure patterns. The approaches considered are discussed in the following paragraphs.

(1) The first attempt to arrive at a suitable approach was based on the following assumptions (refer to Fig. 1 for nomenclature):

1. A wedge of soil under the footing is assumed to remain rigid and to move with the footing (defined by sides making an angle of  $\phi$  with the horizontal surface for footings with a rough base).
2. The failure surface is a segment of a circle from the apex of the wedge to the surface.
3. The center of the failure circle is located arbitrarily at a distance  $y$  above the surface and at a horizontal distance  $x$  from the centerline of the footing.
4. The failure circle associated with the lowest failure load,  $P$ , is assumed to be the most nearly correct circle.
5. The failure is symmetrical about the centerline of the footing.
6. The full cohesive stress is developed in the soil along the failure surface.

ARMOUR RESEARCH FOUNDATION OF ILLINOIS INSTITUTE OF TECHNOLOGY

7. The frictional force along the failure arc is governed by the cohesion and the weight above each point.

These assumptions can be justified for static conditions in at least two ways: first, the resulting failure surfaces are similar to those postulated by Terzaghi for a rough based footing<sup>1/</sup>, and, second, the failure surfaces are similar to those obtained from footings on Ottawa sand<sup>2/</sup>. These justifications are by no means introduced to prove that the assumed failure pattern is correct. It is, however, felt that the assumed failure pattern will be a reasonable representation for the observed pattern<sup>2/</sup>. Also, since no other assumption, including Terzaghi's<sup>1/</sup>, is completely in agreement with the observed patterns, one might expect the assumptions made here to provide essentially the same bearing capacity as Terzaghi's solution for static loads.

(2) The second approach represents a modification of Hill's plasticity solution (see Appendix A). For this approach, no wedge is assumed under the footing, and the failure pattern is as indicated on Fig. 2. If one considers this failure mode as two mirror-image footings exhibiting one-sided failure, the approach used in the original program for one-sided failure (based on Andersen's<sup>3/</sup> failure surface) is directly applicable. If the footing is considered as half the width, the one-sided failure load can be doubled to obtain the bearing capacity for the original footing. The nature of this approach is so similar to that used earlier for one-sided failure that detailed consideration is not required. Plots of  $P$  versus  $B$  or  $r$  versus  $B$  could be easily prepared for various soil properties as was done earlier.<sup>4/</sup> In considering this approach it should be kept in mind that in the experimental phases of this program wedges are observed under the footing.

(3) The plasticity solution for the punch on the half space (Prandtl's solution) can also be used directly. Figure B.3 (Appendix B) shows the velocity field associated with the Prandtl solution. Such a failure mode could be used directly as a basis for predicting symmetrical failure.

---

<sup>1/</sup> Terzaghi, K. and Peck, R. B., Soil Mechanics in Engineering Practice, John Wiley and Sons, Inc., New York, 1948, p. 168.

<sup>2/</sup> McKee, K. E., Op. Cit., Appendix C

<sup>3/</sup> Andersen, P., Op. Cit., p. 81

<sup>4/</sup> McKee, K. E., Op. Cit., Appendix E

These three approaches should be considered only as examples of the many failure patterns which might be postulated. Although some consideration has been given to each of the three approaches, they are limited by their common assumptions. Detailed research in this area will be conducted when, and if, it is justified by the experimental results. For the present, the aim was to consider some possible method of treating two-sided failure with the same general type of engineering approach used earlier for one-sided failure.

It may be well to consider some of the limitations implied in the above approaches, with emphasis on the observed experimental results. The failure mode under dynamic loads may be the same as for static loads, i.e., a clearly defined failure surface, but the experimental results for Ottawa sand indicate that such a failure mode may form for dynamic loads only when displacements are much greater than would be associated with their formation under static loads. This indicates that the failure mode may differ from the idealized assumptions discussed above through at least part of the displacement. The actual resistance-displacement is not rigid-plastic for static loads, and there is no reason to assume that it would be under dynamic conditions. The other elements of the assumptions similarly must be subjected to critical evaluation before they can be accepted. Suffice it to say, that there are many questions which only the evaluation of the experimental results can answer.

#### D. Non-Vertical Loads

In the original program, attention was devoted primarily to footings subjected to vertical forces. This is an extremely common type of loading, and for this reason it can be expected to be important. There are, however, other types of loads which do occur alone or in combination with the vertical loads: (1) overturning moments, (2) inclined loads, and (3) torsional moments. The last of these is of little practical importance and will not be considered in this report.

Overturning moments can be treated by considering eccentric loads, i.e., combinations of direct vertical load and overturning moments. By introducing the same assumptions used in the original analysis for one-sided failure, this problem can be analyzed. The analysis for this class of loading is given in detail in Appendix C. Since the treatment there is complete, suffice it

to say that the graphical results presented in Appendix E of the final report<sup>1/</sup> can be used with only superficial modifications. It should be noted that for this purpose the one-sided failure mode represents the actual behavior.

The influence of inclined loads has been studied during the present program, but to date the results are not satisfactory. It is anticipated that further consideration will result in more suitable analytic approaches and furthermore should allow for a suitable form of presentation. At the time of this writing, the need for a method of treating footings subjected to inclined loads is pointed out, and the fact that work has been and will be done in this respect is reported.

---

<sup>1/</sup> McKee, K. E., Op. Cit.

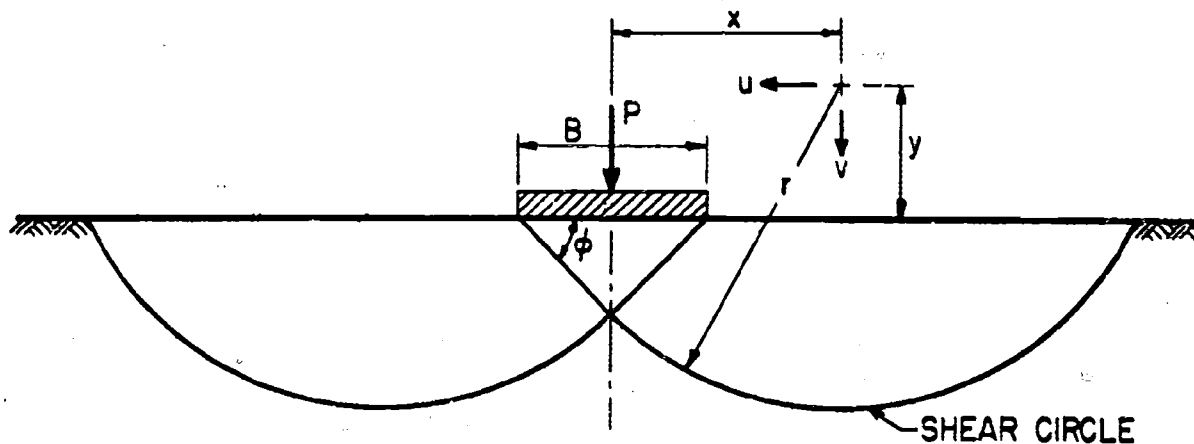


Fig. 1 SIMPLIFIED TWO-SIDED FAILURE MODE BASED ON PRANDTL'S SOLUTION

- B = footing width
- P = vertical load
- x = horizontal distance to center of shear circle from  $\phi$  footing
- y = vertical distance to center of shear circle from ground surface
- r = radius of shear circle
- u,v = horizontal and vertical coordinates measured from center of shear circle.
- $\phi$  = angle of internal friction of soil
- c = cohesion of soil
- $\gamma$  = unit weight of soil

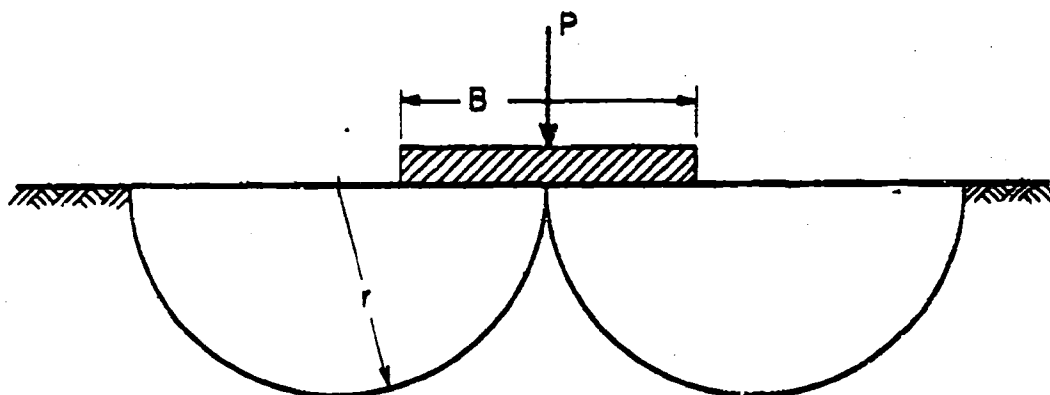


Fig. 2 SIMPLIFIED TWO-SIDED FAILURE MODE BASED ON HILL'S SOLUTION

## Chapter 3

### EXPERIMENTAL INVESTIGATION

#### A. General

The scope of this project includes laboratory experimentation to verify and support the theoretical research. This chapter discusses the planned experimental studies and reports on the results obtained thus far. Since the laboratory work was initiated during June, the experimental results are, of necessity, limited, and in some cases only preliminary results are available. In the following sections, the experimental studies will be considered in three phases: material properties, two-dimensional experiments in the glass box, and three-dimensional experiments in the sand box. The planning for each of these phases will be discussed with detailed information reported in the appendices.

#### B. Material Properties

Material property studies fall into two categories: standard classification tests required as part of the over-all experimental program and special research intended to increase the available knowledge regarding the properties of dense sand. The first is an adjunct to the experimental research and requires no special justification. Suffice it to say, that standard soil classification tests will be conducted, supplemented by additional special tests as may prove desirable. The second category consists of special studies intended to provide detailed soil properties. Appendix D reports on laboratory work dealing with Ottawa sand. The angle of internal friction,  $\phi$ , found in the triaxial tests of the original program was questioned since it differed significantly from that computed from bearing formulas based on the footing tests conducted in the laboratory. Improved experimental procedures have provided data regarding the angle of internal friction -- data which appears to correlate with the results of the footing tests. Also included in Appendix D are the results of a series of experiments dealing with restraints at the interface between sand and glass or sand and steel. These studies are intended to provide relative and absolute information for use in the glass box (two-dimensional experiments).

ARMOUR RESEARCH FOUNDATION OF ILLINOIS INSTITUTE OF TECHNOLOGY

For the initial laboratory studies involving cohesive soils, it was decided to use one of the manufactured soils that have been investigated under ARF sponsorship<sup>1/</sup>. By combining natural soil constituents under controlled conditions it has been found possible to produce soils having consistent properties suitable for experimental studies.

C. Two-Dimensional Studies

A glass-sided container has been used to simulate two-dimensional conditions. Static and dynamic tests have been conducted on loose and dense Ottawa sand, and the manufactured cohesive material. Static loads were applied through a hydraulic jack or by means of a controlled strain rate apparatus. Dynamic loads were applied using the apparatus developed on this program (see Appendix G). Complete records were made, and Fastox photographs were taken of the soil-footing interaction under dynamic loads. Details of these experiments are contained in Appendix E.

D. Three-Dimensional Studies

A box having plan dimensions of 4 ft by 4 ft and a depth of 3 ft was used for three-dimensional footing tests. The only material utilized to date has been Ottawa sand. This same material was used in the original program, thus, the results of the static experiments conducted in the original program are applicable. Details of the three-dimensional dynamic experiments are reported in Appendix F.

---

<sup>1/</sup> Selig, E. T., and Rowe, R. D., Artificial Soils, Armour Research Foundation, K920, September 1960.



## Chapter 4

### CONCLUSIONS

This interim report has attempted to cover all the research conducted during the first half of the contract period. In general, the reported work is in progress, and as a result complete data and generalizations based on the research are lacking. Thus, the conclusions and recommendations expressed below are tentative and subject to later revision.

The partnership of theoretical and experimental research applied on this project has proved most effective. Parallel development in these two directions has maximized the information which has been obtained within the scope of the research. The availability of experimental results has lead to the elimination of several 'promising' theoretical approaches, while at the same time observations have provided the concepts for other analytical techniques.

The studies to date have provided much information regarding footing behavior. The studies relating to behavior under static loads verify, in general, the classical shear surface approaches. One-sided and symmetrical failure surfaces have been observed. The bearing capacities have been correlated with those determined from the applicable theories. Earlier incongruities, between the soil properties determined from triaxial tests and those required to correlate the theories and experiments, have been resolved. All indications are that triaxial or direct shear tests conducted on the same soil and at the same density would result in soil properties satisfying the theoretical requirements.

The original project<sup>1/</sup> considered only one type of dynamic load -- the dropped weight. These experiments were carried out to establish the potential of conducting dynamic experiments on small footings, but due to project limitations, recording was limited to visual and photographic observations before and after the load application. From these observations of footings in both the sand box and the glass box, there was no indication of the formation of a shear surface under a single load application. (The second and third drops on the same footing were sufficient to cause shear

---

<sup>1/</sup> McKee, K. E., Op. Cit.

failure.) This failure mode, i.e., settlement without observable shear surfaces under dynamic loading caused by a single dropping of a weight, would be quite different from that observed at the same deflection for a static load. This 'different' behavior could be at least intuitively explained, since the dropped weight represents a relatively extreme dynamic load -- essentially an initial impulse. On the other hand, it could be argued that a drop from a sufficient height would cause shear surfaces to form and hence that the behavior would be similar to that for static loads.

The development of the dynamic loading apparatus on the current project has allowed the application of less extreme type of dynamic loads. The results of such tests indicate that shear surfaces would form although the associated displacements exceed those for static load. This implies that the more extreme the type of dynamic load, the greater the difference in behavior, (in the case of a linearly decreasing load-time history, extremity would be associated with high peak loads and short durations). It might further be speculated that the difference in behavior is associated with the displacement at which failure surfaces form.

Appendix A

APPLICATION OF PLASTICITY AND LIMIT ANALYSIS  
TO FOOTING DESIGN

by R. L. Chiapetta

ARMOUR RESEARCH FOUNDATION OF ILLINOIS INSTITUTE OF TECHNOLOGY

Appendix A  
APPLICATION OF PLASTICITY AND LIMIT ANALYSIS  
TO FOOTING DESIGN

by R. L. Chiapetta

A.1 Introduction

The objective of this appendix is to consider the role of the theory of plasticity and limit analysis as tools for investigating the behavior of footings. The behavior of footings subjected to static loads will be discussed with particular attention to the difficulties involved in obtaining a solution and some of the limitations of the methods. This will be followed by a presentation of results of past studies of the static problem. Consideration of the dynamic problem is contained in Appendix B. Explicitly, the discussion will be mainly restricted to consideration of continuous footings subject to vertical loads. It is assumed that the footing is rigid relative to the soil, so that the footing may be considered as a rigid punch.

The difficulty in determining the behavior of a footing subjected to either static or dynamic loads stems, in part, from the complex mechanical properties of real soils. For simplicity, the soil properties are idealized to permit use of mathematical theories, such as the theories of elasticity and plasticity. Both of these theories may be applied to the footing response problem. Unfortunately, the theory of elasticity, at times, has been employed where its validity is questionable. This is due in part to the absence of an adequate formulation of a rule for determining the validity of the theory. The following "rule of thumb" for the applicability of elastic theory in soil mechanics problems has been suggested (1)<sup>1/</sup>. If the factor of safety of a mass of soil with respect to failure by plastic flow (continuous deformation at a constant state of stress) exceeds a value of about 3, the vertical stresses in the soil can be estimated by the theory of elasticity.

---

<sup>1/</sup> Numbers in parenthesis refer to references listed in Section A.7.

## A.2 Plasticity Theory

In this appendix, failure is defined such that in some portion of the soil the stress level is high enough to extend into the "plastic" range. It is further assumed that the stresses at a point are related according to an accepted failure theory. For failure, it is expected that, in general, three types of zones in the soil will have to be considered: elastic zones where the stresses can be computed by elastic theory, plastic zones where the state of stress may be determined by using equations of plasticity, and transition zones of intermediate states of stress. The existence of transition zones makes the problem of computing the stresses extremely complicated. In order to simplify the analysis, the existence of transition zones is sometimes disregarded, and the soil is referred to as an elastic-plastic material. Although some work has been conducted on work-hardening<sup>1/</sup> theories for soil mechanics (2), the theories have not been developed to the point of general acceptability. For this reason it is usually assumed that the material is perfectly plastic.<sup>2/</sup>

The field equations of plasticity consist of equilibrium equations, strain-displacement equations, stress-strain relations, and the yield function. An exact solution to a plasticity problem consists of a stress field and a corresponding strain or displacement field related by the stress-strain relations. The stresses must satisfy the equilibrium equations, the yield function, and boundary conditions on the stresses. The compatible displacements must satisfy specified displacement boundary conditions.

The equilibrium and strain-displacement equations are of the same form as in the theory of elasticity. However, in plasticity the total strains appearing in the strain-displacement relations are composed of the sum of the elastic and plastic strains (3). The elastic strains are related to the stresses by the stress-strain relations of linear elasticity. The usual assumptions of perfect plasticity require the stress-plastic strain rate

---

<sup>1/</sup> A work-hardening material is one for which increased stress accompanies increased strain in the plastic range.

<sup>2/</sup> A perfectly plastic material is one for which the strain will increase under constant stress.

relation to be of the form

$$\epsilon'_{ij}{}^P = \lambda \frac{\partial F(\sigma_{ij})}{\partial \sigma_{ij}}, \quad (A.1)$$

where the  $\epsilon'_{ij}{}^P$  are the components of the plastic strain rates,  $\sigma_{ij}$  are the corresponding components of stress,  $F$  is the yield function, and  $\lambda$  is a positive factor of proportionality which may be a function of the space coordinates (4).

In two-dimensional soil mechanics, Coulomb's formula (1) for the yield function is usually assumed. This function reduces to the Tresca or von Mises function when the angle of internal friction is equal to zero. With reference to three dimensions, the Coulomb failure law for an ideal cohesive soil has been used to obtain the yield surface representing the yield function (5). Modified Tresca and von Mises yield functions, which are dependent on mean normal stress, have been considered as proper generalizations of the Coulomb rule to three dimensions which reduce to the Coulomb law for two dimensions (6). An important feature of a perfectly plastic material, that obeys Coulomb's failure theory, is that it exhibits dilatancy, that is, plastic deformation must be accompanied by an increase in volume (8). It should be noted that, in fact, dilatancy is observed in many soils, such as dense sand or stiff clay.

For the problem of a rigid punch on a semi-infinite mass of soil, only the incipient plastic flow problem is usually considered in the literature, so that the boundary conditions at the undeformed surface are satisfied (7). Determining the stresses and velocities, after the punch has penetrated a finite distance, is more difficult and would require a study of the successive phases of the plastic flow. A consideration of the static problem of footings is helpful in gaining insight into and is a necessary prelude to the study of the corresponding dynamic problem.

The case of a continuous footing reduces to a plane strain problem. In general, for an elastic-perfectly plastic material three ranges of mechanical behavior are present in a plane strain problem: the elastic range (below the elastic limit), the range of contained plastic deformation (between the elastic limit and the flow limit), and the range of unrestricted plastic flow (beyond

the flow limit). Many plane strain problems have been solved by the theory of elasticity, but analytical solution for the entire range of contained plastic deformation has generally been possible only when the shape of the elastic-plastic boundary was known a priori from symmetry conditions. As a rule, the shape of the elastic-plastic boundary is not known beforehand and general methods of solving such problems have not been developed (3). An additional complication is that the stress boundary conditions are not generally sufficient to make the problem statically determinate.

Because of these difficulties, contained plastic deformations can seldom be treated by exact analysis, and it is necessary to consider numerical methods such as have been successfully used in the case of elastic-plastic torsion. However, locating the elastic-plastic boundary by numerical techniques is much more difficult in plane strain than in torsion (3). Although a stress function describes the stress distribution in both cases, the stress components are given by the first derivatives in the case of torsion, but by the second derivatives in the case of plane strain. In both cases, the elastic-plastic boundary is located by the condition that discontinuities of stress cannot exist across this boundary. In the case of torsion this means that the stress function and its first derivative should be continuous across the elastic-plastic boundary. However, for plane strain, the stress function and its first and second derivatives must be continuous. To fulfill the condition of continuity at the elastic-plastic boundary, a much finer mesh must be used in problems of plane strain than is necessary in torsion problems. This can be expected to complicate the numerical work considerably.

The final state of unrestricted plastic flow usually cannot be treated in plane strain problems without a full analysis of the preceding states of contained plastic deformation. The analysis of the contained plastic deformation would be necessary to locate the boundary between the elastic and plastic regions. In the problem of torsion of bars, it is possible to treat the final state of unrestricted plastic flow without reference to the preceding elastic-plastic states since such flow can occur only when the entire bar has become plastic (3).

### A.3 Limit Theories

If one is interested in the loads necessary to cause unrestricted elastic flow and not particularly interested in the exact stress distribution at failure, the theorems of limit design (9) can be a great aid. It should be noted that the theorems are valid for three-dimensional problems as well as for those of plane strain. The theorems of limit design are concerned with bodies of perfectly plastic material subject to arbitrary histories of loading that are completely specified. It is assumed that the boundary conditions are of the stress type, that is, at every point of the body each component of the surface traction is specified except where the corresponding component of displacement is prescribed to be zero.

Before quoting the theorems, it may be well to define some concepts and terms involved in the statement of the theorems:

A perfectly plastic material is completely characterized by its yield function  $F$ , which, for a homogeneous material, is only explicitly dependent on the nine stress components. States of stress within the elastic range,  $0 < F < 1$ , are called safe. Plastic flow can occur only under states of stress for which  $F = 1$ . States of stresses for which  $F > 1$  are not possible in a perfectly plastic material.

The term collapse in the theorems refers to conditions for which plastic flow would occur under constant loads if the accompanying change in the geometry of the structure or body were disregarded. For this type of collapse, the equilibrium conditions can be set up for the undeformed body.

Statically admissible stress fields are defined as states of stress for which the components of the stress tensor are continuous functions satisfying the conditions of static equilibrium throughout the body and on those portions of the boundary where the components of the surface tractions are given. The preceding definition may be generalized to include stress fields with a finite number of surfaces of discontinuity. In these cases, the stresses must satisfy the conditions of equilibrium on either side of such a surface and the components of the surface tractions must be continuous across the discontinuity surface.

A kinematically admissible velocity field must satisfy two basic requirements. First, the velocity component must vanish on those portions of the surface where the corresponding components of the surface tractions are not prescribed, and secondly, the rate at which the actual surface tractions and body forces do work, based on this velocity field, must equal or exceed the rate of internal dissipation of energy computed from the strain rates treated as purely plastic strain rates.



Subject to the above assumptions and definitions the following two theorems are valid: I. If a safe statically admissible state of stress can be found at each stage of loading, collapse will not occur under the given loading history. II. If a kinematically admissible collapse state can be found at any stage of loading, collapse must be impending or must have taken place previously. These theorems can be used to provide an upper and lower bound on conditions at collapse. The bounds so established may be sufficiently close for engineering usage. In some cases, as will be mentioned later, the upper and lower bounds can be made to coincide, thus the exact collapse condition is determined.

In the above definition of a kinematically admissible velocity field, no mention is made of continuity. The concept of a discontinuity in the velocity field often is very useful in applying the limit theorems. A velocity discontinuity is simply an idealization of a continuous distribution in which the velocity changes very rapidly across a thin transition layer. If the yield function depends on the mean normal stress (as it does in Coulomb's failure theory), a discontinuity in tangential velocity must be accompanied by a separation or discontinuity in normal velocity. In such a case, the actual transition layer must have appreciable thickness, but the concept of a discontinuity surface still may be useful for purposes of calculation.

The above limit theorems are valid in the presence of a transition layer and are therefore valid in the limit as the thickness of the transition layer approaches zero, provided that the rate of dissipation of energy in the transition layer approaches a finite limit (9).

A very simple type of velocity field that is often used for establishing a kinematically admissible field is a rigid body sliding between two portions of the soil mass. This of course implies a discontinuity in velocity at the interface of relative motion. This type of discontinuity will be called a "slide" discontinuity. As was previously mentioned, for a material whose yield function depends on the mean normal stress, a discontinuity in tangential velocity requires an accompanying normal or separation velocity. For a slide discontinuity in a Coulomb soil, the angle between the

resultant velocity vector and the tangent to discontinuity surface is equal to the angle of internal friction. This condition restricts the types of admissible "slide" discontinuity surfaces to be either a plane (translation) or logarithmic spiral (rotation). For a material whose yield function is independent of the mean normal stress, such as the von Mises yield function, the permissible slide discontinuity surfaces are planes and segments of circles. An example of the use of a plane velocity discontinuity surface will be given later, in the problem of determining an upper bound on the critical height of an unsupported vertical bank of soil.

Discontinuous states of stress as well as discontinuous velocity fields are permissible in the application of the limit theorems. Discontinuous stress fields are of special value when used to obtain lower bounds on the quantities at collapse, even though the stress fields may be without physical significance (10). Equilibrium considerations require that normal and shear stress be continuous across a line of stress discontinuity, but the tangential stress may be discontinuous. It can be shown that a failure line cannot be a line of discontinuity in the stresses and since a discontinuity in the velocity can only occur across a failure line (10), it follows that the velocity field must be continuous across a line of stress discontinuity.

It has been shown (11) that the limit theorems previously stated for assemblages of perfectly plastic bodies do not always apply when there is finite sliding friction at the common interfaces, such as might be present at the contact area of the rigid footing and the soil mass in the classical two-dimensional footing problem. Since the displacement or velocity vector makes an angle equal to the angle of internal friction with the sliding surface, there is a force acting normal to the surface, and work is done, therefore, against the normal force. It is this negative work which gives rise to trouble in the upper bound theorem. The rate of internal dissipation cannot be calculated in all cases because frictional dissipation is not uniquely determined by the flow pattern. It depends not only on relative displacement rate but also on the normal pressure on the frictional interface, a quantity which will often not be known. This type of difficulty does not affect the lower bound theorem.

Theorems have been developed (11) which relate the limit loads with finite Coulomb friction to the extreme cases of zero friction or of complete attachment. The theorems are stated as follows: A. Any set of loads that produce collapse for the condition of no relative motion at the interfaces will produce collapse for the case of finite friction. B. Any set of loads that will not cause collapse when all the coefficients of friction are zero will not cause collapse with any values of the coefficients.

Occasionally these theorems enable the limit load to be computed precisely for finite non-zero friction. The well known two-dimensional footing problem (which will be discussed later) for a von Mises material provides such an example. Two solutions are available for upper bound computations. One by Prandtl (12) contains a rigid region which acts as an extension of the punch and the contact area. The other by Hill (13) assumes zero friction, and appreciable slip does take place. Both solutions give the same answer for the average pressure  $(2 + \pi) k$  where  $k$  is the yield stress in simple shear. This value also has been shown to be a lower bound. Therefore, the limit pressure is  $(2 + \pi) k$  for all possible values of the coefficient of friction.

It should be noted that while the limit theorems are valid for an elastic-perfectly plastic material, the elastic strains are not considered when establishing a kinematically admissible velocity field. Therefore, the material can be considered to be rigid-perfectly plastic<sup>1/</sup> for the purpose of determining bounds on the collapse load; for a rigid-perfectly plastic material, as well for an elastic-perfectly plastic material, three groups of differential equations describe the behavior of the material, namely the stress equilibrium equations, the stress-strain relations, and the strain-displacement relationships. In general, an infinity of stress states will satisfy the stress boundary conditions, the equilibrium equations, and the yield criterion; and an infinite number of displacement fields compatible with a continuous distortion can be found, independent of the stresses, which satisfy the displacement boundary conditions. The stress-strain relations

---

<sup>1/</sup> A rigid-perfectly plastic material is one which undergoes no strain until the plastic state is reached, in which deformation occurs at a constant state of stress.

are necessary to determine states of stress and displacement that correspond. In elasticity theory, a unique solution of stresses and displacements exists, however, there is not unique solution for a rigid-plastic material. The solutions normally presented consist of a deformation mode valid for the entire body considered and a corresponding stress state for the region containing the plastically deforming material. The completeness of such a solution depends on whether it is possible to find a stress solution, satisfying the boundary conditions and equilibrium equations for the region assumed to be rigid, that does not violate the yield conditions. These partial solutions have been referred to as "incomplete" solutions and the ones for which the stress solution has been extended to the whole body concerned are called "complete" solutions (14).

The velocity fields associated with incomplete solutions are used to establish kinematically admissible fields, and hence they furnish upper bound values. The complete solutions for stress and deformations, while they are indeed acceptable solutions for a rigid plastic material, cannot be regarded as the limit to the solution for a real material whose rigidity constants have become infinite. Nevertheless, the collapse loads associated with these solutions are the actual collapse loads for an elastic material with infinite moduli (rigid-plastic) or for that matter finite moduli (elastic-plastic). The relationship of the deformation modes obtained in complete solutions to those for an elastic-plastic material (14) is unknown.

#### A.4 Previous Studies

Several studies have been made which illustrate well the application of the limit theorems to the determination of bounds on the collapse load of a footing. In these studies, the weight of the material has been neglected in the stress equilibrium equations. Investigations regarding the influence of the weight of the mass have not passed beyond the stage of establishing the differential equations (1). The weight of the material complicates the situation considerably. At given values of cohesion and angle of internal friction, the material weight increases the critical load and changes the shape of the surfaces of sliding within the plastic regions of the material. The problem of computing the critical load on the assumption that the unit

weight is greater than zero has been solved only by approximate methods (1).

The above mentioned studies are based on the solutions proposed by Prandtl and Hill or generalizations thereof. Prandtl (12) proposed a stress field at incipient flow for the plane strain problem of a flat rigid punch on a semi-infinite mass of rigid-perfectly plastic material which obeys Coulomb's yield function. The stress field was given only for the plastic portion of the mass in the immediate vicinity of the punch. No stress solution was presented for the rigid region away from the punch. The velocity field associated with the stress field implies that the punch was rough, that no relative motion occurs between the punch and the contact area. The bearing pressure corresponding to the stress field is

$$p = c \cot \phi \left[ 1 + \pi \tan \phi \tan^2 \left( \frac{\pi}{4} + \frac{\phi}{2} \right) - 1 \right] , \quad (A.2)$$

where  $c$  is the cohesion and  $\phi$  is the angle of internal friction in Coulomb's law.

Hill (13) later also proposed a stress solution for the same problem for the special case where  $\phi = 0$  (Tresca or von Mises function). This stress field resulted in the same bearing pressure as for the Prandtl solution; this pressure is

$$p = (2 + \pi) k , \quad (A.3)$$

where  $k$  is the yield stress in simple shear. Note that Eq.A.2 reduces by use of L'Hospital's rule to Eq.A.3 when  $\phi = 0$ , where  $c$  corresponds to  $k$ . The velocity field associated with Hill's solution implies that the punch is smooth.

Both of these solutions are "incomplete" solutions as defined earlier, and their presentation occurred prior to the development of the upper and lower bound theorems of limit design. However, after publication of the limit theorems, it was shown that the velocity fields associated with Hill's and Prandtl's solutions were kinematically admissible fields (15). Therefore, the pressure value in Eqs.A.2 and A.3 are upper bounds for Coulomb and Tresca materials respectively. In addition, Shield and Drucker (15) used limit analysis to show that a lower bound on the collapse pressure for a Tresca material is  $5 k$ .

ARMOUR RESEARCH FOUNDATION OF ILLINOIS INSTITUTE OF TECHNOLOGY

More recently, Shield (16) has extended the Prandtl stress solution into the rigid region and succeeded in establishing a statically admissible stress field throughout the material for values of  $\phi < 75^\circ$ . Therefore, the Prandtl value, Eq. A.2, is both an upper and lower bound on the collapse pressure for values of  $0 \leq \phi < 75^\circ$ , and hence is the exact value of average collapse pressure.

Shield and Drucker (15) extended the application of limit analysis to the three-dimensional punch problem by considering the problem of a rectangular flat punch on a Tresca material. It was shown that a lower bound for any rectangular punch is again  $5k$  while the upper bound for a smooth punch lies between  $5.71k$  for a square and  $(2 + \pi)k$  for a very long rectangle.

Shield (5) subsequently constructed a yield surface for three-dimensional stress fields based on Coulomb's yield function and used the lower bound theorem of limit analysis to determine a lower bound for the bearing capacity of a smooth or rough rectangular footing on a soil. The stress field was an adaptation of the statically admissible stress field previously used by Shield and Drucker (15) for a Tresca material. The lower bound obtained for the limit pressure was

$$p = \frac{1}{2} c \tan^3 \left( \frac{\pi}{4} - \frac{\phi}{2} \right) \left[ 4 + \sin \phi + \sin^2 \phi + (1 + \sin \phi) (4 + \sin^2 \phi)^{1/2} \right] + 2 c \tan \left( \frac{\pi}{4} + \frac{\phi}{2} \right). \quad (A.4)$$

The limit theorems have also been used in problems related to the classical punch problem, that is, in the problem of the plastic indentation of a layer by a footing. A complete plane strain solution to the problem of plastic flow in a thin sheet of perfectly plastic material laid on a rough base and compressed by a smooth flat footing has already been obtained (17). In addition, through employment of the limit theorems, Shield (17) determined upper and lower bounds on the average indentation pressure for the same problem extended to three dimensions, for a square and circular footing.

Another promising use of the limit design theorems in this area, is in problems with inhomogeneous media (6). They are apt to be of greatest use in such cases because of the enormous difficulty in obtaining exact solutions.

#### A.5 Illustrative Problem

To illustrate the application of the limit design theorems to soil mechanics, the upper and lower bound determination of the critical height of a vertical unsupported bank of soil is presented here. A statically admissible discontinuous equilibrium solution (8) is shown in Fig. A.1, where  $w$  denotes unit weight. As mentioned earlier, a statically admissible stress field must satisfy the equilibrium equations, the yield criterion, and the stress boundary conditions. In addition, since the proposed stress field is discontinuous, the direct stress normal to the discontinuity line and the shear stress parallel to the discontinuity line, must be continuous across it. It is easily seen from Fig. A.1 that these continuity requirements and also the stress boundary conditions (namely, stress free boundaries) are satisfied. It remains to be shown then, that the stress field satisfies equilibrium and the yield criterion in each of the three regions shown in Fig. A.1.

The equilibrium equations are

$$\begin{aligned}\frac{\partial \sigma_x}{\partial x} + \frac{\partial \tau_{xy}}{\partial y} &= 0 \\ \frac{\partial \tau_{xy}}{\partial x} + \frac{\partial \sigma_y}{\partial y} &= -w\end{aligned}\tag{A.5}$$

The first equation is identically satisfied in each region. The first term in the second equation is zero, and the second term is equal to  $-w$  for all three regions. Therefore, both equations are satisfied throughout the entire body.

Coulomb's yield criterion may be expressed as follows:

$$\tau \leq c - \sigma \tan \phi, \quad (\text{A.6})$$

where  $c$  is the cohesion;  $\phi$  is the angle of internal friction;  $\tau$  and  $\sigma$  (taken as positive for tension) are the shearing and normal stress respectively on a failure surface. Alternatively, the failure criterion may be expressed by

$$R \leq c \cos \phi - \frac{\sigma_x + \sigma_y}{2} \sin \phi, \quad (\text{A.7})$$

where  $R$  is the maximum shearing stress at a point. The maximum shearing stress in Region I is  $wH/2$  and occurs at the lower ground level. In Region II, the maximum shearing stress is equal at every point and is also  $wH/2$ . The plane maximum shearing stress is zero everywhere in Region III. Therefore, the yield criterion is satisfied in Region I if

$$\frac{wH}{2} \leq c \cos \phi - \frac{-wH}{2} \sin \phi$$

or

(A.8)

$$H \leq \frac{2}{w} \frac{c \cos \phi}{(1 - \sin \phi)}.$$

In Region II, the following inequality must hold for all values of  $y$ ,

$$\frac{wH}{2} \leq c \cos \phi - \frac{-2wy + wH}{2} \sin \phi$$

or

$$\frac{wH}{2} (1 + \sin \phi) - wy \sin \phi \leq c \cos \phi.$$

Note that if this inequality is valid for  $y = H$ , then it is valid for all values of  $y$  in Region II. Therefore, setting  $y = H$  the above inequality may be rewritten as

$$H \leq \frac{2}{w} \frac{c \cos \phi}{(1 - \sin \phi)}, \quad (\text{A.9})$$



which is identical to Eq.A.8. This may be written as

$$H = \frac{2c}{w} \tan \left( \frac{\pi}{4} + \frac{\phi}{2} \right) . \quad (A.10)$$

In Region III, the condition to be met is that

$$0 \leq c \cos \phi - \frac{2w(y-H)}{2} \sin \phi$$

or

$$(H - y) \leq \frac{c}{w} \cot \phi ,$$

which is satisfied for all values of  $y$  in Region III; hence, this inequality provides no real restriction on  $H$ .

Therefore, if the condition of Eq.A.10 is satisfied, the stress field in Fig.A.1 is statically admissible and a lower bound on the critical height is given by Eq.A.10.

A velocity field with a rigid-body slide discontinuity is shown in Fig. A.2. We shall now proceed to prove that it is kinematically admissible. One of the requirements for a kinematically admissible field was that the velocity component be zero on those portions of the surface where the corresponding component of the surface traction is not prescribed. However, in this problem the surface tractions are prescribed on the entire surface, and therefore this requirement is automatically satisfied.

Furthermore, in previous discussion, it was stated that for a discontinuity in tangential velocity, such as is proposed in Fig. A.2, the angle between the resultant relative velocity vector and the discontinuity surface is equal to  $\phi$ , the angle of internal friction. Therefore, the normal and tangential velocities must be related by

$$\partial v' = \partial u' \tan \phi , \quad (A.11)$$

as is shown in Fig. A.2, where  $\partial v'$  and  $\partial u'$  denote the normal and tangential velocities respectively.

The only remaining requirement for a kinematically admissible velocity field is that the rate at which the actual surface tractions and body forces do work based on the proposed velocity field, must equal or exceed the rate of dissipation of internal energy computed from the strain rates treated as purely plastic strain rates.

The surface tractions do no work since they are prescribed to be zero. The rate at which the body forces (weight) do work is

$$\frac{1}{2} w H^2 \tan \beta [\partial u' \cos \beta - \partial v' \sin \beta] .$$

From Eq.A.11, this can be written in the form

$$\frac{1}{2} w H^2 \tan \beta [\partial u' \cos \phi - \tan \phi \sin \phi] . \quad (A.12)$$

Dissipation of internal energy takes place only at the surface of sliding since the sliding body is rigid. The rate of dissipation of energy per unit area of surface is given by the expression

$$D = \tau \partial u' + \sigma \partial v' . \quad (A.13)$$

With Eq.A.6 and A.11 this equation reduces to

$$D = c \partial u' . \quad (A.14)$$

The total rate of dissipation is obtained by multiplying  $D$  by the length of the line of discontinuity,  $H/\cos \beta$ , therefore

$$c \partial u' H/\cos \beta \quad (A.15)$$

is the total rate. The requirement for a kinematically admissible field is that the expression in Eq.A.12 must be greater or equal to the expression in Eq.A.15, hence

$$\frac{1}{2} w H \tan \beta [\cos \beta - \tan \phi \sin \beta] \geq c/\cos \beta$$

or

$$\frac{1}{2} w H \sin \beta [\cos \phi \cos \beta - \sin \phi \sin \beta] - c \cos \phi = 0 .$$

This reduces to

$$H \geq \frac{2 c \cos \phi}{w \sin \beta \cos (\phi + \beta)} \quad (A.16)$$

Minimizing the right-hand side gives

$$\beta = \frac{\pi}{4} - \frac{\phi}{2} .$$

Therefore,

$$H \geq \frac{2 c \cos \phi}{w \sin \left( \frac{\pi}{4} - \frac{\phi}{2} \right) \cos \left( \frac{\pi}{4} + \frac{\phi}{2} \right)}$$

or

(A.17)

$$H \geq \frac{4 c}{w} \tan \left( \frac{\pi}{4} + \frac{\phi}{2} \right) .$$

provides an upper bound on the critical height,  $H_c$ . Note, from Eq.A.10 and A.17, there is a factor of two between the upper and lower bound,

$$\frac{2 c}{w} \tan \left( \frac{\pi}{4} + \frac{\phi}{2} \right) \leq H_c \leq \frac{4 c}{w} \tan \left( \frac{\pi}{4} + \frac{\phi}{2} \right) . \quad (A.18)$$

The upper bound can be improved by considering a rotational discontinuity (logarithmic spiral) instead of the translational type, however the translational type equally well illustrates the method.

#### A.6 Dynamic Problem

Although the limit theorems provide a very useful tool for determining bounds on the static collapse load, no such general methods are available for the case of dynamic loading. A numerical procedure can of course be employed, however the addition of inertia terms in the governing equations will certainly add to the complexity of the problem and may necessitate more simplifying assumptions than introduced in the static problem. The plane plastic strain problem with inertial effects is discussed in detail in the following appendix.

## A.7 References

1. K. Terzaghi, Theoretical Soil Mechanics, John Wiley and Sons, 1943.
2. D. C. Drucker, R. E. Gibson, and D. J. Henkel, "Soil Mechanics and Work-Hardening Theories of Plasticity", Proc. ASCE, Vol. 81, Paper 798, Sept. 1955.
3. W. Prager and P. G. Hodge, Theory of Perfectly Plastic Solids, John Wiley and Sons, 1951.
4. D. C. Drucker, "Some Implications of Work-Hardening and Ideal Plasticity", Q. Appl. Math., 7 (1950), 411-418.
5. R. T. Shield, "On Coulomb's Law of Failure in Soils", J. Mech. Phys. Solids, 4 (1955), 10-16.
6. D. C. Drucker, "Limit Analysis of Two- and Three-Dimensional Soil Mechanics Problems", J. Mech. Phys. Solids, 1 (1953), 217-226.
7. R. T. Shield, "Mixed Boundary Value Problems in Soil Mechanics", J. Mech. Phys. Solids, 11 (1953), 61-75.
8. D. C. Drucker and W. Prager, "Soil Mechanics and Plastic Analysis or Limit Design", Q. Appl. Math., 10 (1952), 157-165.
9. D. C. Drucker, W. Prager, and H. J. Greenberg, "Extended Limit Design Theorems for Continuous Media", Q. Appl. Math., 9 (1952), 381-389.
10. R. T. Shield, "Stress and Velocity Fields in Soil Mechanics", J. Math. Phys. 33, 2 (1954), 144-156.
11. D. C. Drucker, "Coulomb Friction, Plasticity, and Limit Loads", J. Appl. Mech., 21 (1954), 71-74.
12. L. Prandtl, "Über die Harte plastischer Körper", Goettinger Nachr., Math.-Phys. Kl., (1920), 74-85.
13. R. Hill, "The Plastic Yielding of Notched Bars Under Tension", Q. J. Mech. Appl. Math., 2 (1949), 40-52.
14. J. F. W. Bishop, "On the Complete Solution to Problems of Deformation of a Plastic Rigid Material", J. Mech. Phys. Solids, 2 (1953), 43-53.
15. R. T. Shield, and D. C. Drucker, "The Application of Limit Analysis to Punch-Indentation Problems", J. Appl. Mech., 20 (1953), 453-460.
16. R. T. Shield, "Plastic Potential Theory and Prandtl Bearing Capacity Solution", J. Appl. Mech., 21 (1954), 193-194.
17. R. T. Shield, "The Plastic Indentation of a Layer by a Flat Punch", Q. Appl. Math., 13 (1955), 27-46.

ARMOUR RESEARCH FOUNDATION OF ILLINOIS INSTITUTE OF TECHNOLOGY

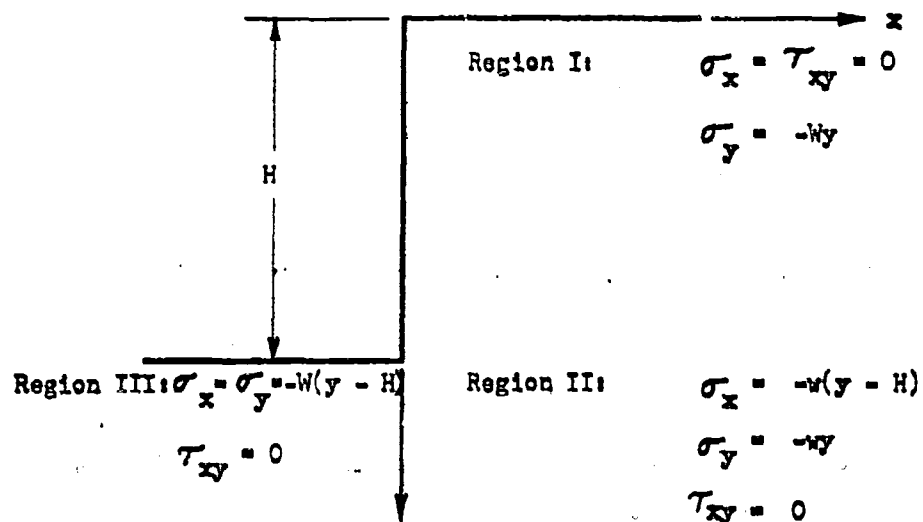


Fig. A.1 AN EQUILIBRIUM SOLUTION

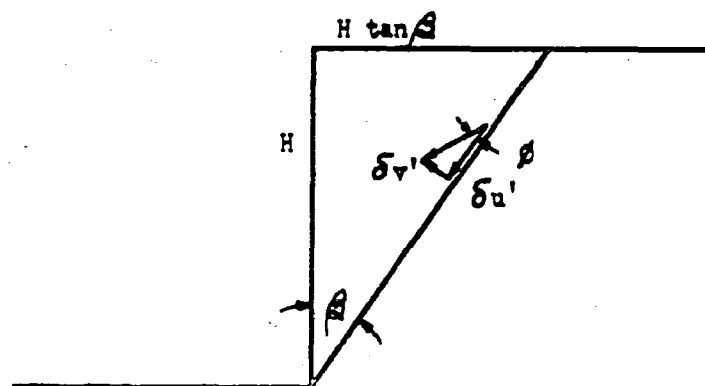


Fig. A.2 A VELOCITY SOLUTION

Appendix B

THE METHOD OF CHARACTERISTICS  
APPLIED TO PROBLEMS OF PLANE PLASTIC STRAIN  
WITH INERTIAL EFFECTS

by Philip G. Hodge, Jr.

ARMOUR RESEARCH FOUNDATION OF ILLINOIS INSTITUTE OF TECHNOLOGY

Appendix B  
THE METHOD OF CHARACTERISTICS  
APPLIED TO PROBLEMS OF PLANE PLASTIC STRAIN  
WITH INERTIAL EFFECTS

by Philip G. Hodge, Jr.

B.1 Introduction

If a slowly increasing load is applied to a structure made of a rigid-perfectly plastic material, the structure will remain rigid so long as the load remains less than a certain critical load variously known as the "yield-point load", "collapse load", or "limit load". If the yield-point load is reached and maintained for a finite length of time, the structure will deform in a quasi-static flow, which will continue indefinitely or until the geometry of the structure is sufficiently changed so that the yield-point load of the deformed structure is different from that of the original structure. However, if the load is increased above the yield-point load, there will be no possible equilibrium configuration of stresses and all or part of the structure will engage in accelerated plastic flow. In conventional applications, such accelerated plastic flow would be disastrous to the structure, and its theoretical details are generally of little practical interest. However, if the time duration of the overload is sufficiently small, then the inertial resistance may be great enough to limit the deformations to structurally reasonable values. The relation of this type of loading to blasts from nuclear or H E detonations is obvious.

Previous work on overloads of this type has been done on beam and frame type structures, (1- 15),<sup>1/</sup> circular plates (16 - 19) and circular cylindrical shells (20 - 26) . The present appendix is concerned with problems in which the plastic structure is in a state of plane strain. A typical problem in this category is that of a semi-infinite plastic mass pressed upon by a rigid punch. (The term "structure" is perhaps used loosely here, referring as it does to the semi-infinite plastic mass.) Such problems have

---

<sup>1/</sup> Numbers in parantheses refer to the references listed at the end of the appendix.

been previously treated from the quasi-static viewpoint (see, for example, 27 or 28 for text-book treatments) but this is believed to be the first attempt to include inertial effects in a problem of plane strain.

In the next section, we shall first state the basic differential equations of the problem and simplify them somewhat by a change of variables. We shall then find the characteristics of this system and the relations that must hold along these characteristics. This discussion will be carried out for deformations of arbitrary magnitude. Section B.3 will begin with simplification of the equations for the case of small deformations such that the Eulerian and Lagrangian coordinates need not be distinguished from each other. The differential equations will then be replaced by corresponding difference equations in preparation for a numerical solution. The following section will be concerned with the example mentioned above in which a rigid punch is pressed against a semi-infinite plastic mass. A possible numerical scheme for the solution of this example will be presented. Finally, the report will conclude with some suggestions for extension of the results, both to other problems of plane strain and to some related problems in soil mechanics.

## B.2 Basic Equations

Under the usual assumptions of plane strain, three stress components,  $\sigma'_x$ ,  $\sigma'_y$ ,  $\tau'_{xy}$ , and two velocity components,  $u'$  and  $v'$  must be determined. Primes are used to denote physically dimensioned quantities; unprimed symbols will presently be introduced for corresponding dimensionless quantities. To determine these quantities, we have available two equations of motion

$$\frac{\partial \sigma'_x}{\partial x'} + \frac{\partial \tau'_{xy}}{\partial y'} = \rho \frac{Du'}{Dt} \equiv \rho \left[ \frac{\partial u'}{\partial t'} + u' \frac{\partial u'}{\partial x'} + v' \frac{\partial u'}{\partial y'} \right] \quad (a)$$

$$\frac{\partial \sigma'_y}{\partial y'} + \frac{\partial \tau'_{xy}}{\partial x'} = \rho \frac{Dv'}{Dt} \equiv \rho \left[ \frac{\partial v'}{\partial t'} + u' \frac{\partial v'}{\partial x'} + v' \frac{\partial v'}{\partial y'} \right] \quad (b)$$



the yield condition,

$$F(\sigma'_x, \sigma'_y, \tau'_{xy}) \equiv (\sigma'_x - \sigma'_y)^2 + 4(\tau'_{xy})^2 - 4k^2 = 0 \quad (c)$$

(B.1)

and three flow-law equations,

$$\epsilon_x \equiv \frac{\partial u'}{\partial x'} = \lambda' \frac{\partial F}{\partial \sigma'_x} \equiv 2 \lambda' (\sigma'_x - \sigma'_y) \quad (d)$$

$$\epsilon_y \equiv \frac{\partial v'}{\partial y'} = \lambda' \frac{\partial F}{\partial \sigma'_y} \equiv 2 \lambda' (\sigma'_y - \sigma'_x) \quad (e)$$

$$\tau_{xy} \equiv \frac{\partial u'}{\partial y'} + \frac{\partial v'}{\partial x'} = \lambda' \frac{\partial F}{\partial \tau'_{xy}} \equiv 8 \lambda' \tau'_{xy} \quad (f)$$

Here  $\lambda'$  is an unknown scalar function that represents the magnitude of the plastic strain-rate tensor. We introduce dimensionless quantities defined by

$$x' = Lx, \quad y' = Ly, \quad u' = \sqrt{2k/\rho} u, \quad v' = \sqrt{2k/\rho} v \quad (B.2)$$

$$\sigma'_x = 2k\sigma_x, \quad \sigma'_y = 2k\sigma_y, \quad \tau'_{xy} = 2k\tau_{xy}, \quad t' = L\sqrt{\rho/2k} t$$

where  $L$  is a typical length of the problem, so that Eq B.1 become

$$\frac{\partial \sigma_x}{\partial x} + \frac{\partial \tau_{xy}}{\partial y} = \frac{\partial u}{\partial t} + u \frac{\partial u}{\partial x} + v \frac{\partial u}{\partial y} \quad (a)$$

$$\frac{\partial \sigma_y}{\partial y} + \frac{\partial \tau_{xy}}{\partial x} = \frac{\partial v}{\partial t} + u \frac{\partial v}{\partial x} + v \frac{\partial v}{\partial y} \quad (b)$$

$$(\sigma_x - \sigma_y)^2 + 4\tau_{xy}^2 - 1 = 0 \quad (c) \quad (B.3)$$

$$\frac{\partial u}{\partial x} = \lambda (\sigma_x - \sigma_y) \quad (d)$$

ARMOUR RESEARCH FOUNDATION OF ILLINOIS INSTITUTE OF TECHNOLOGY

$$\frac{\partial v}{\partial y} = \lambda (\sigma_y - \sigma_x) \quad (e)$$

$$\frac{\partial u}{\partial y} + \frac{\partial v}{\partial x} = 4 \lambda \tau_{xy} \quad (f)$$

Next, define  $\omega$  as the dimensionless mean normal stress and  $\theta$  as the angle from the negative  $y$  axis to the first shear direction (see 27), which leads to

$$\begin{aligned} \sigma_x &= \sigma'_x / 2k = \omega + \frac{1}{2} \sin 2\theta \\ \sigma_y &= \sigma'_y / 2k = \omega - \frac{1}{2} \sin 2\theta \\ \tau_{xy} &= \tau'_{xy} / 2k = -\frac{1}{2} \cos 2\theta \end{aligned} \quad (B.4)$$

Equations B.4 identically satisfy Eq. B.3. At the same time, we combine Eq. B.3, B.3d, e, and f so as to eliminate  $\lambda$ . The resulting set of four equations for the unknowns  $\omega$ ,  $\theta$ ,  $u$ , and  $v$  is

$$\omega_x + \theta_x \cos 2\theta + \theta_y \sin 2\theta - u u_x - v v_y = u_t \quad (a)$$

$$\omega_y + \theta_x \sin 2\theta - \theta_y \cos 2\theta - u v_x - v v_y = v_t \quad (b)$$

(B.5)

$$u_x + v_y = 0 \quad (c)$$

$$u_x \cos 2\theta + u_y \sin 2\theta + v_x \sin 2\theta - v_y \cos 2\theta = 0, \quad (d)$$

where subscripts are now used to indicate differentiation.

The explicit time dependence of the problem occurs only in the right-hand sides of Eq. B.5. For the purpose of finding the characteristic curves at any time  $t$  of Eq. B.5, we may temporarily regard the right-hand sides as known. The characteristic curves are then defined as those curves

$\Gamma$  across which some derivatives of  $\omega$ ,  $\theta$ ,  $u$ , and/or  $v$  may be discontinuous; although the functions themselves are continuous. If  $\omega$  is known along such a curve  $\Gamma$ , then the variation  $d\omega$  along  $\Gamma$  is also known. Therefore, the partial derivatives of  $\omega$  on  $\Gamma$  must satisfy

$$\omega_x dx + \omega_y dy = d\omega. \quad (a)$$

Similar relations must hold for the other variables: (B.6)

$$\theta_x dx + \theta_y dy = d\theta \quad (b)$$

$$u_x dx + u_y dy = du \quad (c)$$

$$v_x dx + v_y dy = dv. \quad (d)$$

In general, the eight Eq. B.5 and B.6, regarded as linear algebraic equations for the eight derivatives  $\omega_x$ ,  $\omega_y$ ,  $\theta_x$ ,  $\theta_y$ ,  $u_x$ ,  $u_y$ ,  $v_x$ ,  $v_y$  will yield a unique solution. However, a characteristic curve is defined by the property that these derivatives are not all unique, but may have different values on the two sides of the curve. The condition for this lack of uniqueness is that the determinant of coefficients vanish:

$$\begin{vmatrix} 1 & 0 & \cos 2\theta & \sin 2\theta & -u & -v & 0 & 0 \\ 0 & 1 & \sin 2\theta & -\cos 2\theta & 0 & 0 & -u & -v \\ 0 & 0 & 0 & 0 & 1 & 0 & 0 & 1 \\ 0 & 0 & 0 & 0 & \cos 2\theta & \sin 2\theta & \sin 2\theta & -\cos 2\theta \\ dx & dy & 0 & 0 & 0 & 0 & 0 & 0 \\ 0 & 0 & dx & dy & 0 & 0 & 0 & 0 \\ 0 & 0 & 0 & 0 & dx & dy & 0 & 0 \\ 0 & 0 & 0 & 0 & 0 & 0 & dx & dy \end{vmatrix} = 0 \quad (B.7)$$

After some manipulation, this requirement can be shown to be equivalent to the equation

$$\left[ \sin 2\theta \left( \frac{dy}{dx} \right)^2 + 2 \cos 2\theta \left( \frac{dy}{dx} \right) - \sin 2\theta \right]^2 = 0 \quad (\text{B.8})$$

Therefore, Eq. B.8 represents the desired differential equation for the characteristic curves of Eq. B.5. Solving for  $\frac{dy}{dx}$ , we see that

$$\frac{dy}{dx} = -\cot \theta \quad (\text{a})$$

(B.9)

$$\frac{dy}{dx} = \tan \theta \quad (\text{b})$$

are each double characteristics of Eq. B.5; we denote them as first and second characteristics, respectively. In view of the geometric interpretation of  $\theta$ , the characteristic curves are everywhere in the directions of the lines of principal shearing stress.

The preceding results are identical with those obtained for the corresponding quasi-static problem (27, 28). To obtain the relations which must hold along the characteristics, we refer Eq. B.5 to curvilinear coordinates  $\xi$  and  $\eta$  in the first and second characteristic directions, respectively (Fig. B.1). Denoting the components of the velocity vector by  $\mu$  and  $\nu$  in the  $\xi$  and  $\eta$  directions, respectively, we may write

$$\begin{aligned} d\xi &= \sin \theta \, dx - \cos \theta \, dy; & u &= \mu \sin \theta + \nu \cos \theta \\ d\eta &= \cos \theta \, dx + \sin \theta \, dy; & v &= -\mu \cos \theta + \nu \sin \theta \end{aligned} \quad (\text{B.10})$$

Substitution of Eq. B.10 into B.5 together with some elementary manipulation leads eventually to the four equations

$$\mu_{,\eta} - \nu \theta_{,\eta} = 0 \quad (\text{a})$$

(B.11)

$$\nu_{,\xi} + \mu \theta_{,\xi} = 0 \quad (\text{b})$$

$$(\omega - \theta)_\xi = \dot{\nu}(\mu_\eta - \dot{\nu}\theta_\eta) + (\mu_\epsilon - \dot{\nu}\theta_\epsilon) \quad (c)$$

$$(\omega + \theta)_\eta = \mu(\dot{\nu}_\xi + \mu\theta_\xi) + (\dot{\nu}_\epsilon + \mu\theta_\epsilon) \quad (d)$$

The terms on the right-hand sides of Eq.B.11c and d are, of course, the inertial effects. If they vanish, Eq B.11 reduce to the well-known results for quasi-static plasticity.

### B.3 Difference Equations for Small Deformations

If the total deformations are sufficiently small, we need no longer distinguish between Eulerian and Lagrangian coordinates. Thus, regarding the left-hand sides of Eq.B.1b and c as written in Eulerian coordinates, we may use the simple time derivate of the middle members rather than the extreme right-hand sides of Eq.B.1a and b. Following this argument through, we find that the non-linear velocity terms in Eq.B.11c and d have disappeared so that our set of equations is now

$$\mu_\xi - \dot{\nu}\theta_\xi = 0 \quad (a)$$

$$\dot{\nu}_\eta + \mu\theta_\eta = 0 \quad (b)$$

(B.12)

$$(\omega - \theta)_\xi = \mu_\epsilon - \dot{\nu}\theta_\epsilon \quad (c)$$

$$(\omega + \theta)_\eta = \dot{\nu}_\epsilon + \mu\theta_\epsilon \quad (d)$$

To replace Eq.B.12 by difference equations, we consider first derivatives with respect to time. At any instant  $t$ , we may reasonable assume that we have solved the problem for all previous times, in particular, at a time  $t - \Delta t$ . If we expand any function  $\phi$  at  $t - \Delta t$  in a Taylor's series about  $t$  we obtain

$$\varphi(t - \Delta t) = \varphi(t) - \varphi_t(t) \Delta t + \frac{1}{2} \varphi_{tt}(t) \Delta t^2 + \dots$$

Therefore,

(B.13)

$$\varphi_k(t) = \frac{\varphi - \bar{\varphi}}{\Delta t} + k \Delta t,$$

where  $k \Delta t$  represents the error involved in truncating the series and the notation  $\bar{\varphi}$  is used to designate  $\varphi(t - \Delta t)$ .

Replacing the time derivatives in Eq. B.1 by Eq. B.13, we obtain the set of equations

$$\mu_j - \nu \theta_j = 0 \quad (a)$$

$$\nu_n + \mu \theta_n = 0 \quad (b)$$

(B.14)

$$(\omega - \theta)_j = \frac{(\mu - \bar{\mu}) - \nu(\theta - \bar{\theta})}{\Delta t} + k \Delta t \quad (c)$$

$$(\omega + \theta)_n = \frac{(\nu - \bar{\nu}) + \mu(\theta - \bar{\theta})}{\Delta t} + k \Delta t \quad (d)$$

To replace derivatives with respect to  $\xi$  and  $\eta$  by finite differences, we express the values at the mesh points by Taylor's series about the midpoints A or B in Fig. B.2. Thus

$$\left. \begin{array}{l} \varphi_{i+1/2} \\ \varphi_{i-1/2} \end{array} \right\} = \varphi(A) \pm \frac{1}{2} \Delta \xi_{i-1/2} \varphi_{\xi}(A) + \frac{1}{8} \Delta \xi_{i-1/2}^2 \varphi_{\xi\xi}(A) \pm \frac{1}{48} \Delta \xi_{i-1/2}^3 \varphi_{\xi\xi\xi}(A) + \dots$$

whence, by adding or subtracting,

$$\varphi(A) = \frac{1}{2} (\varphi_{i-1/2} + \varphi_{i+1/2}) + k \Delta \xi_{i-1/2}^2 \quad (a)$$

$$\Delta \xi_{i-1/2} \varphi_{\xi}(A) = \varphi_{i+1/2} - \varphi_{i-1/2} + k \Delta \xi_{i-1/2}^3 \quad (b)$$

(B.15)

Similarly,

$$\phi(B) = \frac{1}{2} (\phi_{i,j-1} + \phi_{ij}) + k \Delta \eta_{ij}^2 \quad (c)$$

$$\Delta \eta_{ij} \phi_{\eta}(B) = \phi_{i,j-1} + k \Delta \eta_{ij}^3 \quad (d)$$

Substitution of Eq.B.15 into Eq.B.14 yields the four difference equations

$$\mu_{i-1,j} - \mu_{ij} - \frac{1}{2} (\nu_{i-1,j} + \nu_{ij}) (\theta_{i-1,j} - \theta_{ij}) + k \Delta \xi^2 = 0 \quad (a)$$

$$\nu_{i,j-1} - \nu_{ij} + \frac{1}{2} (\mu_{i,j-1} + \mu_{ij}) (\theta_{i,j-1} - \theta_{ij}) + k \Delta \xi^2 = 0 \quad (B.16)$$

(b)

$$\begin{aligned} & (\omega_{i-1,j} - \theta_{i-1,j}) - (\omega_{ij} - \theta_{ij}) + k_1 \Delta t \Delta \xi + k_2 \Delta \xi^2 = \\ & = \frac{1}{2} [(\mu_{i-1,j} + \mu_{ij} - \bar{\mu}_{i-1,j} - \bar{\mu}_{ij}) / \Delta t + \\ & - \frac{1}{2} (\nu_{i-1,j} + \nu_{ij}) (\theta_{i-1,j} + \theta_{ij} - \bar{\theta}_{i-1,j} - \bar{\theta}_{ij})] \Delta \xi_{ij} / \Delta t \end{aligned} \quad (a)$$

$$(\omega_{i,j-1} + \theta_{i,j-1}) - (\omega_{ij} + \theta_{ij}) + k_1 \Delta t \Delta \eta + k_2 \Delta \eta^2 = \quad (B.17)$$

$$\begin{aligned} & = \frac{1}{2} [(\nu_{i,j-1} + \nu_{ij} - \bar{\nu}_{i,j-1} - \bar{\nu}_{ij}) + \\ & + \frac{1}{2} (\mu_{i,j-1} + \mu_{ij}) (\theta_{i,j-1} + \theta_{ij} - \bar{\theta}_{i,j-1} - \bar{\theta}_{ij})] \Delta \eta_{ij} / \Delta t \end{aligned} \quad (b)$$

In the application to follow,  $\mu$  and  $\nu$  will generally be known at points to the left and below and it will be necessary to propagate up and to the right. Therefore, we are interested in solving Eq.B.16 for  $\mu_{ij}$  and  $\nu_{ij}$  in terms of values at  $i-1, j$  and  $i, j-1$ . To this end, we simply replace  $i$  by  $i-1$  in Eq.B.16a and  $j$  by  $j-1$  in Eq.B.16b. Doing this, and solving the resulting linear relations explicitly for  $\mu_{ij}$  and  $\nu_{ij}$ , we obtain

$$\begin{aligned} \mu_{ij} = & \left[ \mu_{i-1,j} - \frac{1}{4} \mu_{i,j-1} (\theta_{ij} - \theta_{i-1,j}) (\theta_{ij} - \theta_{i,j-1}) + \right. \\ & \left. + \frac{1}{2} (\nu_{i-1,j} + \nu_{i,j-1}) (\theta_{ij} - \theta_{i-1,j}) \right] / \left[ 1 + \frac{1}{4} (\theta_{ij} - \theta_{i-1,j}) (\theta_{ij} - \theta_{i,j-1}) \right] \end{aligned} \quad (B.18)$$

$$\begin{aligned} \nu_{ij} = & \left[ \nu_{i,j-1} - \frac{1}{4} (\theta_{ij} - \theta_{i,j-1})(\theta_{ij} - \theta_{i,j-1}) \nu_{i,j-1} \right. \\ & \left. - \frac{1}{2} (\mu_{i,j-1} + \mu_{i,j}) (\theta_{ij} - \theta_{i,j-1}) \right] / \left[ 1 + \frac{1}{4} (\theta_{ij} - \theta_{i,j-1})(\theta_{ij} - \theta_{i,j-1}) \right] \end{aligned} \quad (\text{B.19})$$

To handle the terms  $\Delta \xi_{ij}$  and  $\Delta \eta_{ij}$  in Eq. B.17 we need the geometric relations the Cartesian coordinates  $x_{ij}$ ,  $y_{ij}$ . By use of appropriate power series expansions, it is readily verified that

$$\begin{aligned} x_{i,j-1} - x_{ij} &= \frac{1}{2} \Delta \xi_{ij} (\sin \theta_{i,j-1} + \sin \theta_{ij}) + k \Delta \xi^3 \\ y_{i,j-1} - y_{ij} &= -\frac{1}{2} \Delta \xi_{ij} (\cos \theta_{i,j-1} + \cos \theta_{ij}) + k \Delta \xi^3 \\ x_{i,j-1} - x_{ij} &= \frac{1}{2} \Delta \eta_{ij} (\cos \theta_{i,j-1} + \cos \theta_{ij}) + k \Delta \eta^3 \\ y_{i,j-1} - y_{ij} &= \frac{1}{2} \Delta \eta_{ij} (\sin \theta_{i,j-1} + \sin \theta_{ij}) + k \Delta \eta^3 \end{aligned} \quad (\text{B.20})$$

Solving these relations for  $x_{ij}$ ,  $y_{ij}$ ,  $\Delta \xi_{ij}$  and  $\Delta \eta_{ij}$ , we obtain

$$\begin{aligned} \Delta \xi_{ij} = & 2 A_{ij} \left[ (\sin \theta_{i,j-1} + \sin \theta_{ij})(x_{i,j-1} - x_{i,j-1}) + \right. \\ & \left. - (\cos \theta_{i,j-1} + \cos \theta_{ij})(y_{i,j-1} - y_{i,j-1}) \right] \quad (\text{a}) \quad (\text{B.21}) \end{aligned}$$

$$\begin{aligned} \Delta \eta_{ij} = & -2 A_{ij} \left[ (\cos \theta_{i,j-1} + \cos \theta_{ij})(x_{i,j-1} - x_{i,j-1}) + \right. \\ & \left. + (\sin \theta_{i,j-1} + \sin \theta_{ij})(y_{i,j-1} - y_{i,j-1}) \right] \quad (\text{b}) \end{aligned}$$



$$\begin{aligned}
x_{lj} = A_{lj} & \left[ (\cos \theta_{l,j+1} + \cos \theta_{lj}) (\cos \theta_{l,j+1} + \cos \theta_{lj}) x_{l,j+1} + \right. \\
& + (\sin \theta_{l,j+1} + \sin \theta_{lj}) (\sin \theta_{l,j+1} + \sin \theta_{lj}) x_{l,j+1} + \\
& \left. + (\sin \theta_{l,j+1} + \sin \theta_{lj}) (\cos \theta_{l,j+1} + \cos \theta_{lj}) (y_{l,j+1} - y_{l,j+1}) \right] \quad (B.22)
\end{aligned}$$

$$\begin{aligned}
y_{lj} = A_{lj} & \left[ (\sin \theta_{l,j+1} + \sin \theta_{lj}) (\sin \theta_{l,j+1} + \sin \theta_{lj}) y_{l,j+1} + \right. \\
& + (\cos \theta_{l,j+1} + \cos \theta_{lj}) (\cos \theta_{l,j+1} + \cos \theta_{lj}) y_{l,j+1} + \\
& \left. + (\cos \theta_{l,j+1} + \cos \theta_{lj}) (\sin \theta_{l,j+1} + \sin \theta_{lj}) (x_{l,j+1} - x_{l,j+1}) \right] \quad (B.23)
\end{aligned}$$

where

$$A_{lj} = \left[ 1 + \cos(\theta_{l,j+1} - \theta_{lj}) + \cos(\theta_{l,j+1} - \theta_{lj}) + \cos(\theta_{l,j+1} - \theta_{l,j+1}) \right]^{-1} \quad (B.24)$$

If we subtract Eq B.6b from Eq B.17a and use Eq B.21, we obtain a non-linear algebraic equation which involves only  $\theta$  at the point  $l, j$  :

$$\begin{aligned}
 & [2\theta_y - (\theta_{L,y} + \theta_{L,y}) + \omega_{L,y} - \omega_{L,y}] [1 + \cos(\theta_{L,y} - \theta_y)] + \cos(\theta_y - \theta_{L,y}) + \cos(\theta_{L,y} - \theta_{L,y})] \Delta t = \\
 & = [(\mu_{L,y} + \mu_{L,y} - \bar{\mu}_{L,y}) - \frac{1}{2}(\nu_{L,y} + \nu_{L,y})(\theta_{L,y} + \theta_y - \theta_{L,y} - \theta_y)] \cdot \\
 & \cdot [(\sin \theta_{L,y} + \sin \theta_y)(x_{L,y} - x_{L,y}) - (\cos \theta_{L,y} + \cos \theta_y)(y_{L,y} - y_{L,y})] + \\
 & + [(\nu_{L,y} + \nu_{L,y} - \bar{\nu}_{L,y}) + \frac{1}{2}(\mu_{L,y} + \mu_{L,y})(\theta_y + \theta_{L,y} - \bar{\theta}_{L,y} - \bar{\theta}_{L,y})] \cdot \\
 & \cdot [(\cos \theta_{L,y} + \cos \theta_y)(x_{L,y} - x_{L,y}) + (\sin \theta_{L,y} + \sin \theta_y)(y_{L,y} - y_{L,y})] \\
 & \quad \quad \quad (B.25)
 \end{aligned}$$

Finally, substitution of Eq B.10 into Eq B.6a provides and equation for  $\omega_y$  in terms of known quantities:

$$\begin{aligned}
 \omega_y & = \omega_{L,y} - \theta_{L,y} + \theta_y + \\
 & - [(\mu_{L,y} + \mu_y - \bar{\mu}_{L,y}) - \frac{1}{2}(\nu_{L,y} + \nu_y)(\theta_{L,y} + \theta_y - \theta_{L,y} - \theta_y)] \cdot \\
 & \cdot [(\sin \theta_y + \sin \theta_{L,y})(x_{L,y} - x_{L,y}) - (\cos \theta_y + \cos \theta_{L,y})(y_{L,y} - y_{L,y})] \cdot \\
 & \cdot [1 + \cos(\theta_{L,y} - \theta_y) + \cos(\theta_{L,y} - \theta_y) + \cos(\theta_{L,y} - \theta_{L,y})]^{-1} (\Delta t)^{-1} \\
 & \quad \quad \quad (B.26)
 \end{aligned}$$

To summarize, we have six equations (Eq. B.18, B.19, B.22, B.23, B.25 and B.26) available at each point  $L, j$  to determine the six variables  $\mu_j$ ,  $v_j$ ,  $x_j$ ,  $y_j$ ,  $\theta_j$  and  $\omega_j$  at each point. We shall demonstrate a possible iterative method for solving a particular problem in the next section.

#### B.4 Example

We consider as an example a rigid punch of width  $2L$  pressed against a plastic half-space with a total force  $2Pk$ . The quasi-static solution (Fig. B.3) to this problem is well known (see, for example 27). If the punch surface is perfectly smooth, then there exist alternative velocity fields (27). To avoid possible ambiguity, we shall assume the punch surface to be rough.

The yield-point load is  $P = 2 + \pi$ , and the incipient velocity field consists of a downward motion of the center section ABA of arbitrary velocity  $\dot{z}$ , together with flow along the characteristics of magnitude  $\dot{z}/\sqrt{2}$  in the remaining plastic regions.

We shall assume that the punch displacement  $z$  is known as a function of time and that

$$z(0) = \dot{z}(0) = 0$$

$$\dot{z}(t) \geq 0 \quad (B.27)$$

$$z(t) = z_0 \ll 1 \quad \text{for all } t > T$$

The last restriction enables us to use the Eulerian form of the equations and to neglect the motion of the boundaries. We wish to find the solution at all times  $t$  and in particular to find the desired force  $P$  as a function of time.

We assume that the solution at any time  $t$  has the general character shown in Fig. B.4. A central curvilinear wedge ABA moves rigidly down with velocity  $\dot{z}$ ; in the region ABC, the second characteristics all pass through the singular point A; the characteristics in ACD have no singular point.

Along the wedge boundary AB, the normal component of velocity must be continuous, hence

$$\mu = \dot{z} \cos \theta \quad \text{on AB} \quad (\text{B.27a})$$

With  $\mu$  known, Eq. B.16b with  $j$  replaced by  $j-1$  yields

$$v_j = v_{l,j-1} + \frac{1}{2} \dot{z} (\cos \theta_{lj} + \cos \theta_{l,j-1}) (\theta_{lj} - \theta_{l,j-1}) \quad \text{on AB} \quad (\text{B.27b})$$

Since  $v$  must vanish at B, Eq. B.2 may be applied to find  $v$  at each point on AB.

On the boundary BCD, the normal velocity component must vanish,

$$v = 0 \quad \text{on BCD} \quad (\text{B.28a})$$

It then follows from Eq. B.11a that

$$\mu = \text{const.} = \dot{z}/\sqrt{2} \quad \text{on BCD} \quad (\text{B.28b})$$

where the constant is evaluated from continuity of  $\mu$  at B.

On AD, no loads are applied, hence it follows from Eq B.4 that

$$\omega = -1/2, \quad \theta = 3\pi/4 \quad \text{on AD} \quad (\text{B.29a, b})$$

Also, since motion of the boundary is neglected

$$y = 0 \quad \text{on AD.} \quad (\text{B.29c})$$

Finally, if we prescribe a uniform spacing of mesh points numbered from the point A,

$$x_l = l \Delta x \quad \text{on AD.} \quad (\text{B.29d})$$

It is convenient to regard the singular point A expanded to the infinitesimal curve A' A'' A''' as indicated in the insert to Fig. B.4. From A'' to A''' the field is not singular and the boundary conditions are the same as B.29. However, along A' A'',  $\theta$  on the  $-l$ th characteristic counting from A'' will be assigned the value

$$\theta_l = (3\pi/4) + l \Delta \phi \quad \text{on A'A''} \quad (\text{B.30a})$$

Of course

$$x = y = 0 \quad \text{on } A'A'' \quad (\text{B.30b,c})$$

so that  $\Delta \phi = 0$  and Eq. B.17a reduces to  $\omega - \theta = \text{constant}$ . Hence,

$$\omega = -1/2 + \epsilon \Delta \phi \quad \text{on } A'A'' \quad (\text{B.30d})$$

Assuming  $\omega$  and  $\theta$  to be known on AB, the force  $P$  is given by

$$P = \int_0^1 (-2\omega + \tan \theta) dx \quad (\text{B.31})$$

an equation which is easily integrated numerically.

To find the solution at any time  $t$ , we assume it known at time  $t - \Delta t$ . We guess a value of  $\theta$  based on its previous values. We divide the unknown angle between the characteristics AB and AC at A into  $m$  equal angles  $\Delta \phi$ , where  $m$  is given and  $\Delta \phi$  is guessed. Similarly, the unknown length AD is divided into a known number of intervals  $n$  of equal but unknown magnitude  $\Delta x$ . Denote the point C by  $O$ ,  $O$  and increase along CD and  $j$  along CA.

Equations B.27 and B.28 show that  $\mu$  and  $\nu$  along AB and BC are completely specified in terms of the guessed values of  $\theta$ . Therefore, the right-hand sides of Eq. B.18 and B.19 are all known and  $\mu_{ij}$  and  $\nu_{ij}$  can be found at points next to the boundaries AB and BCD. Continuing this process, we can find  $\mu$  and  $\nu$  throughout the field.

We next apply Eq. B.25 to a point next to the boundary AD, regarding everything as known except  $\theta_{ij}$ . Determining a corrected value for  $\theta_{ij}$  from the resulting non-linear equation, we can then find  $x_{ij}$ ,  $y_{ij}$ , and  $\omega_{ij}$  from Eq. B.22, B.23 and B.26, respectively. This process can be carried out successively back across the entire field and eventually furnishes corrected values of  $\theta$  in the boundaries AB and ACD.

This new solution is not tested against three criteria: (1) the value of  $\theta$  on AB should not have changed too much from the previous step, (2)  $\theta$  at B should equal  $\pi/4$ , and (3)  $x$  at B should equal -1.

Failure of either or both of the last two criteria calls for corrected guesses for  $\Delta\phi$  and  $\Delta x$ , respectively, and failure of any one or more of the three criteria calls for an iteration of the entire process, using the new values for  $\Theta$ ,  $\Delta\phi$ , and  $\Delta x$ . After a sufficient number of iterations so that all criteria are satisfied, another increment of time is added and the entire process is repeated.

## B.5 Conclusions

The preceding analysis represents a first effort in what is believed to be a new field. Some important theoretical questions remain unanswered, and numerous future problems are suggested.

Among the theoretical questions the primary ones deal with convergence, uniqueness, and the non-linear terms in Eq.B.11c and d. It seems intuitively plausible that the iteration procedure suggested for a particular example in the previous section will converge. However, intuition is no substitute for mathematical rigor, and it would be most desirable to prove this convergence in the most general terms possible.

The question of uniqueness is always a thorny one for a perfectly plastic material. Indeed, in quasi-static problems only the yield-point load is unique, it frequently being possible to construct alternative stress or velocity fields. To the author's knowledge, uniqueness of solutions to dynamic plasticity problems has received no attention as yet.

Finally, among the mathematical questions to be answered, is the disturbing one concerning the non-linear velocity terms in the equations of motion. It will be recalled that the characteristics were defined as those curves across which some of the derivatives with respect to  $\eta$  might be discontinuous. Therefore, it is difficult to accept the appearance of such derivatives in Eq.B.11c. The whole subject of the nature of discontinuities permitted across the characteristics needs to be more fully investigated for equations of higher than second order.

Assuming that the appearance of the  $\frac{\partial}{\partial \eta}$  terms in Eq.B.11c is satisfactorily explained, there still remains the question of how to evaluate the equation. Although finite-difference approximations for cross derivative terms are easily obtained, they apparently give a lower order of accuracy

ARMOUR RESEARCH FOUNDATION OF ILLINOIS INSTITUTE OF TECHNOLOGY

for the same number of points.

Turning next to other related problems, an entire vista opens up. Indeed, any problem for which the quasi-static solution is known would seem to be fair game for a dynamic analysis, e.g., indentation of a plastic mass by a rigid wedge. Looking still further ahead, one can consider rotationally symmetric plastic problems whose quasi-static solutions have been obtained by Shield (29, 30).

Still another direction, and one of considerable practical importance, is the extension to the failure criteria usually used in soil mechanics. Here the yield stress  $k$ , instead of being constant, is a function of  $\omega$ . Thus, Eq B.1c must be replaced by

$$(\sigma'_x - \sigma'_y)^2 + 4(\tau'_{xy})^2 - 4[k(\omega)]^2 = 0 \quad (B.32)$$

Obviously, this modification will affect not only the stress equations, but also the flow law. However, although the resulting equations will certainly be more complicated than Eq.B.5, they should be of the same order and contain the same derivatives. It therefore appears reasonable to hope that the resulting problem, although more complicated, will not be intrinsically more difficult. Since even for the perfectly plastic material, a high-speed computing machine must be resorted to, there may well be no essentially new problems encountered in such a modified analysis.

#### B.6 References

1. E. H. Lee, and P. S. Symonds, "Large Plastic Deformations of Beams under Transverse Impact," J. Appl. Mech., 1952, 308-314.
2. E. W. Parkes, "The Permanent Deformation of a Cantilever Struck Transversely at Its Tip", Proc. Roy. Soc. (London) A228 1955, 462-476.
3. P. S. Symonds, "Dynamic Load Characteristics in Plastic Bending of Beams", J. Appl. Mech. 20, 1953, 475-481.
4. R. H. Owens, and P. S. Symonds, "Plastic Deformations of a Free Ring under Concentrated Dynamic Loading", J. Appl. Mech. 22 1955, 523-529.
5. R. C. Alverson, "Impact with Finite Acceleration Time of Elastic and Elastic-Plastic Beams", J. Appl. Mech. 23, 1956, 411-415.

6. H. H. Bleich, and N. G. Salvadori, "Impulsive Motion of Elastoplastic Beams", Proc. ASCE 79, 1953, 287.
7. M. F. Conroy, "Plastic-Rigid Analysis of Long Beams under Transverse Impact Loading", J. Appl. Mech. 19, 1952, 465-470.
8. M. F. Conroy, "Plastic Deformation of Semi-Infinite Beams Subject to Transverse Impact Loading at the Free End", J. Appl. Mech. 23, 1956, 239-243.
9. B. A. Cotter, and P. S. Symonds, "Plastic Deformation of a Beam Under Impulsive Loading", Proc. ASCE 81, 1955, sep. 675.
10. H. G. Hopkins, "On the Behavior of Infinitely Long Rigid-Plastic Beams Under Transverse Concentrated Load", J. Mech. and Phys. Solids 4, 1955, 38-52.
11. T. J. Mentel, "Plastic Deformations Due to Dynamic Loading of A Beam With an Attached Mass", Can. J. Technol. 33, 1955, 237-255.
12. J. A. Seiler, and P. S. Symonds, "Plastic Deformation in Beams under Distributed Dynamic Loads", J. Appl. Phys. 25, 1954, 556-563.
13. J. A. Seiler, B. A. Cotter, and P. S. Symonds, "Impulsive Loading of Elastic-Plastic Beams", J. Appl. Mech. 23, 1956, 515-521.
14. P. S. Symonds, "Large Plastic Deformations of Beams Under Blast Type Loading", Proc. 2d US Natl. Congr. Appl. Mech., Ann Arbor, 1954, 505-515.
15. P. S. Symonds, and C. F. A. Leth, "Impact of Finite Beams of Ductile Metal", J. Mech. and Phys. Solids, 2, 1954, 92-102.
16. H. G. Hopkins, and W. Prager, "On the Dynamics of Plastic Circular Plates", Z. angew. Math. u. Phys. 5, 1954, 317-330.
17. H. G. Hopkins, "Large Elastic-Plastic Deformation of Built-In Circular Plates Under Uniform Load", Part I -- Theoretical Analysis, DAM Rept., DA 2598-12, Brown University, Providence, Rhode Island, 1954.
18. G. E. Hudson, "A Theory of the Dynamic Plastic Deformation of a Thin Diaphragm", J. Appl. Phys. 22, 1951, 1-11.
19. A. J. Wang, and H. G. Hopkins, "On the Plastic Deformation of Built-In Circular Plates under Impulsive Load", J. Mech. and Phys. Solids 3, 1954, 22-37.
20. P. G. Hodge, Jr., "Impact Pressure Loading of Rigid-Plastic Cylindrical Shells", J. Mech. and Phys. Solids 3, 1955, 176-188.
21. P. G. Hodge, Jr., and B. Paul, "Approximate Yield Conditions in Dynamic Plasticity", Proc. 3d Midwestern Conf. Solid Mech.,



22. P. G. Hodge, Jr., "The Influence of Blast Characteristics on the Final Deformation of Circular Cylindrical Shells", J. Appl. Mech. 23, 1956, 617-624.
23. G. Eason, and R. T. Shield, "Dynamic Loading of Rigid-Plastic Cylindrical Shells", J. Mech. and Phys. Solids 4, 1956, 53-71.
24. E. H. Agababyan, "Stresses in a Tube Under a Sudden Application of a Load", Ukrain. Mat. Zhur. 5, 1953, 325-332.
25. E. H. Agababyan, "Dynamic Extension of a Hollow Cylinder under Conditions of Ideal Plasticity", Ukrain. Mat. Zhur. 7, 1955, 243-252.
26. P. G. Hodge, Jr., "Ultimate Dynamic Load of a Circular Cylindrical Shell", Proc. 2d Midwestern Conf. Solid Mech., Lafayette, 1955, 150-177, 1956.
27. W. Prager, and P. G. Hodge, Jr., Theory of Perfectly Plastic Solids, John Wiley and Sons, Inc., New York, 1951.
28. R. Hill, The Mathematical Theory of Plasticity, Oxford Univ. Press, London, 1950.
29. R. T. Shield, "On the Plastic Flow of Metals Under Conditions of Axial Symmetry", Proc. Roy. Soc. (London), A 233, 1955, 267-287.
30. R. T. Shield, "Plastic Flow in A Converging Conical Channel", J. Mech. Phys. Solids 3, 1955, 246-258.

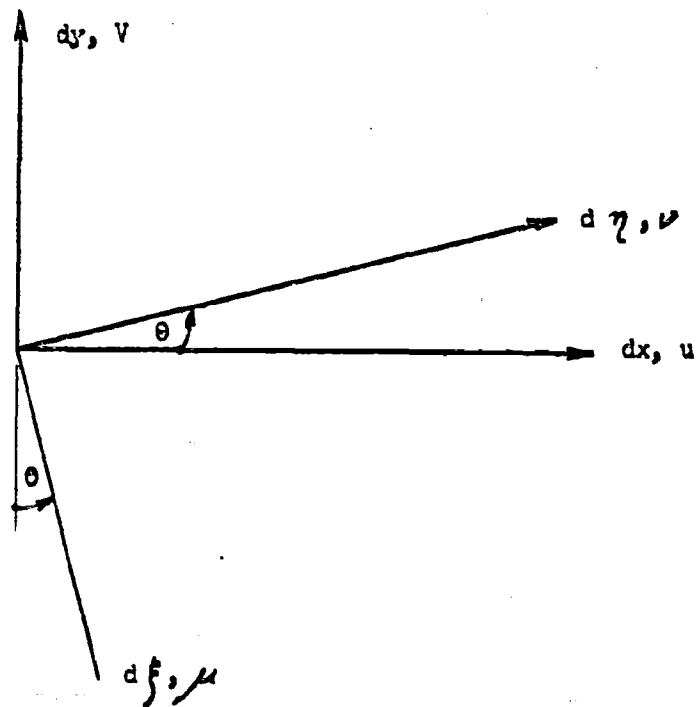


Fig. B.1 CURVILINEAR COORDINATE SYSTEM

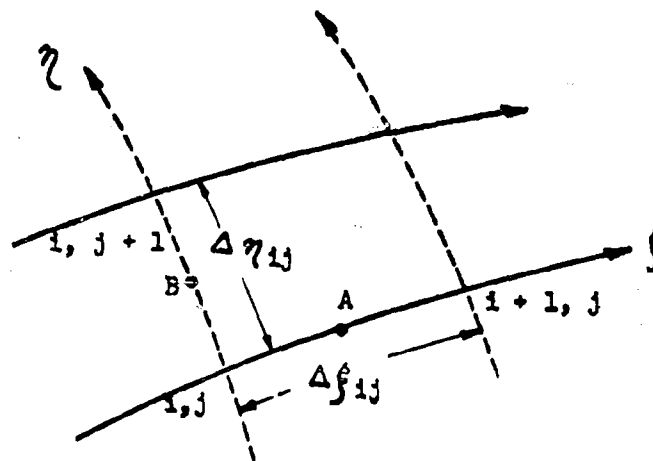


Fig. B.2 TYPICAL MESH IN CHARACTERISTIC NET

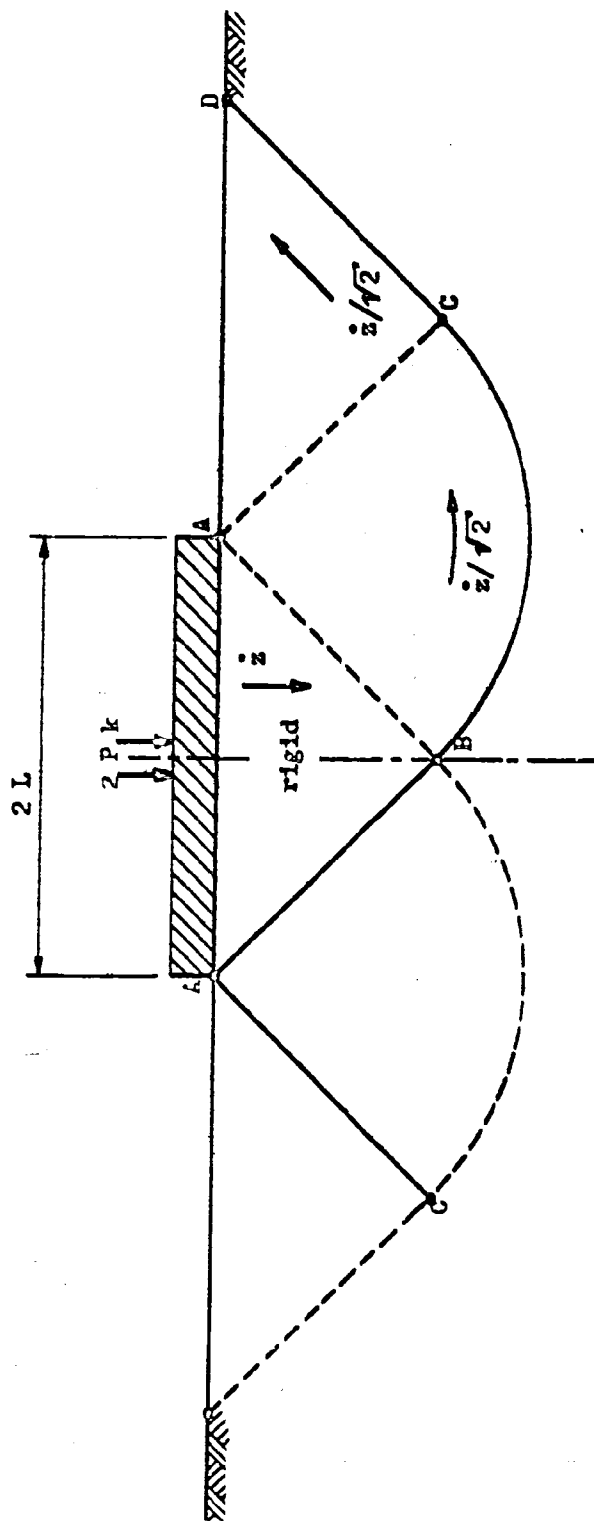


Fig. B.3 PUNCH ON HALF-SPACE: DIMENSIONS AND STATIC SOLUTION

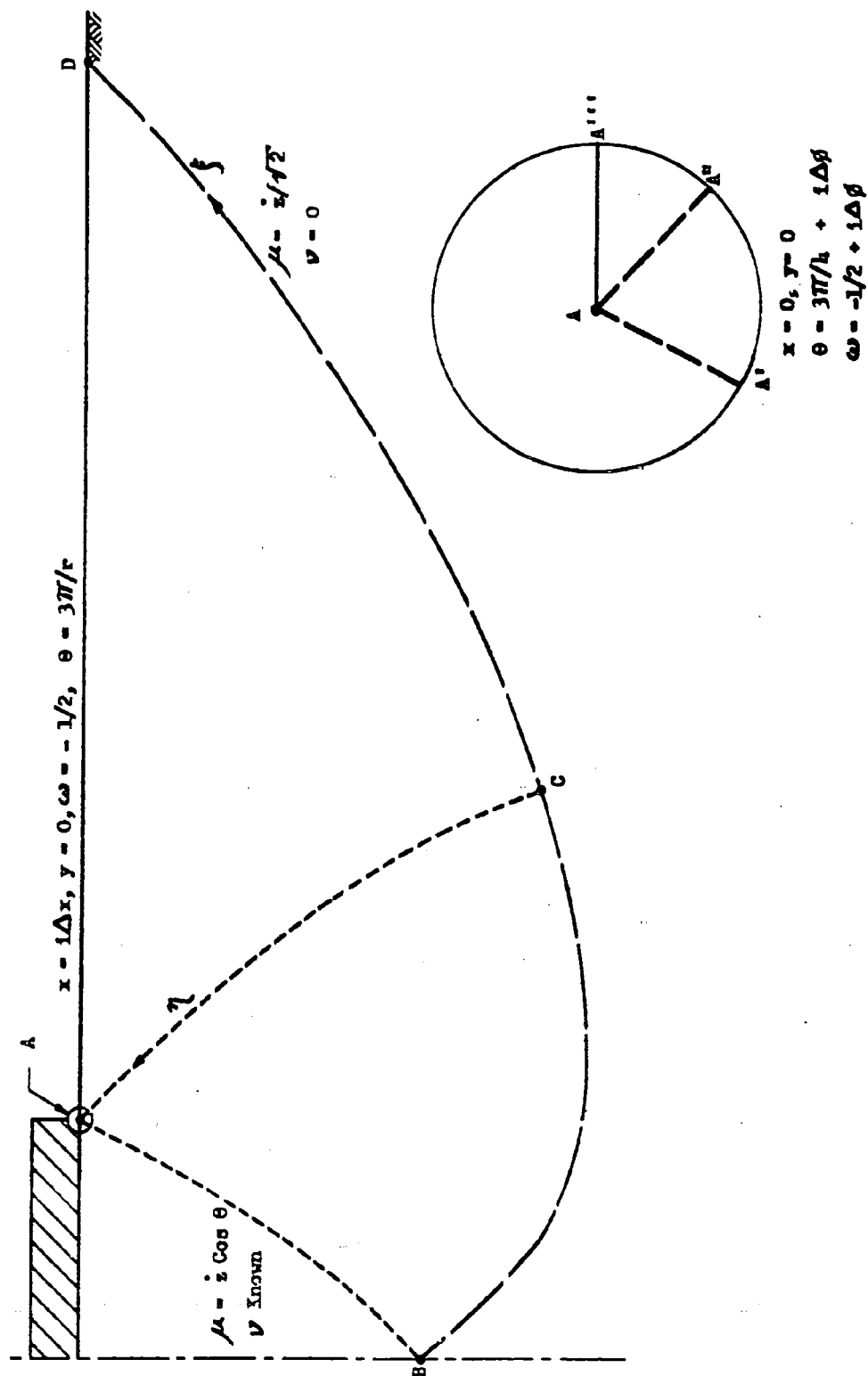


Fig. B.4 PUNCH ON HALF-SPACE: NATURE OF SOLUTION AND BOUNDARY CONDITIONS

Appendix C

FOOTINGS SUBJECTED TO ECCENTRIC LOADS

ARMOUR RESEARCH FOUNDATION OF ILLINOIS INSTITUTE OF TECHNOLOGY

## Appendix C

### FOOTINGS SUBJECTED TO ECCENTRIC LOADS

#### C.1 Introduction

This appendix considers footings subject to eccentric loads, i.e., combinations of direct vertical loads and overturning moments. This loading condition is shown on Fig. C.1, where the moment is  $P_e$ ,  $e$  representing the equivalent eccentricity of the load. Consideration of the possibility of a moment,  $P_e$ , increases the generality of the solutions presented in the Final Report<sup>1/</sup> on the original program. It should be noted that since the case where,  $e = 0$ , reduces to the one-sided failure for central vertical loads as considered earlier, that case ( $e = 0$ ) can be considered as a special class of solutions for the results presented herein.

The assumptions made in this appendix are the same as those made in the original report and represent yet a further extension of Andersen's method<sup>2/</sup>.

1. The failure surface under dynamic loads will be the surface determined by application of the initial value of the dynamic loads as a static load.
2. The resistance offered to movement is rigid plastic in form, i.e., settlement and soil compressibility are not considered.
3. The maximum plastic resistance equals the static resistance determined analytically, associated with the failure surfaces considered in item 1 above.
4. The behavior of the soil is defined by the parameters  $\phi$ ,  $\delta$ , and  $c$ , where  $\phi$  and  $c$  may themselves be functions of many parameters relating to the soil and the condition of loading.

First the static problem will be treated, and then the earlier dynamic approach will be modified to include overturning moments. For the purposes of this appendix, only the resulting equations will be presented -- the development follows that shown in earlier reports on this project.

---

<sup>1/</sup> McKee, K. E., Design and Analysis of Foundations for Protective Structures, AFSWC, TR 59-56, October, 1959.

<sup>2/</sup> Andersen, P., Substructure Analysis and Design, the Ronald Press Co., New York, New York, 1956, p. 81.

## C.2 Static Loads

Based on Fig. C.1, the static solution can be developed for a two-dimensional footing subjected to eccentric loads, following Andersen's general approach. This results in the following two equations:

$$P_s \left[ \frac{4 - \pi \tan \phi}{16 \gamma \tan \phi} \right] = r^2 \left[ 1 + \frac{D}{r} \left( \frac{1 + 2 \tan \phi}{2 \tan \phi} \right) + \left( \frac{D}{r} \right)^2 \left( \frac{1 + 2 \tan \phi}{4 \tan \phi} \right) \right] + \frac{\pi}{4 \gamma} \left[ \frac{c}{\tan \phi} (2r + D) + Dq \left( \frac{r}{D} + \frac{2 + \pi \tan \phi}{2 \pi \tan \phi} \right) \right] \quad (C.1)$$

and

$$\frac{B - 2e}{r} = \left( 2 - \frac{\pi}{2} \tan \phi \right) - \frac{2}{3} \frac{\gamma r^2}{P_s} \left[ (2 \tan \phi - 1) + \left( 1 + \frac{D}{r} \right)^3 (1 + 2 \tan \phi) \right] - \frac{\pi rc}{P_s} \left[ 1 + \frac{q}{2c} \tan \phi \right] \left[ 1 + \left( 1 + \frac{D}{r} \right)^2 \right] - \frac{qD}{P_s} \left( 2 + \frac{D}{r} \right), \quad (C.2)$$

These two equations are comparable to Eq. E.1 and E.2 in the Final Report<sup>1/</sup>. The first equation, C.1, is identical with E.1, while the right-hand side of C.2 is identical with the right-hand side of E.2. Hence, the only influence of the eccentricity is on the left-hand side of Eq. C.2. This allows gross simplification making use of the earlier work. Certainly if  $e = 0$ , the equations are the same and Appendix E<sup>1/</sup> is applicable. Furthermore, when  $e = 0$  the two sets of equations are identical if the quantity  $(B - 2e)$  is used in place of  $B$  in the earlier work. With this substitution in the abscissa, Fig. E.2 through E.26 are applicable. As before, the usefulness of the plotted solutions is limited because it is not practical to plot for all values of  $q$ .

Equations C.1 and C.2, of course, can be solved numerically for any two parameters. For the applications of this project, the parameters that would ordinarily be determined are the ultimate load capacity,  $P_s$ , and the radius of the failure surface,  $r$ . The other parameters: soil

<sup>1/</sup> McKee, K. E., Op. Cit.

properties,  $\phi$  and  $c$ ; footing dimensions,  $B$  and  $D$ ; and eccentricity,  $e$ , would have to be specified. Trial and error solutions are, in general, necessary. The simplest method of solution requires the assumption of a value for  $r$ , which allows direct solution of Eq. C.1 for  $P_g$ . The assumed  $r$  and the computed  $P_g$  can then be substituted into Eq. C.2 to solve for  $B$ . This procedure is repeated as often as required until the desired value of  $B$  is determined, and, hence, the appropriate values of  $P_g$  and  $r$  are established. Extrapolation or interpolation can be used, of course, to find values when nearby values are known.

In the original work for  $e = 0$ , the effect of  $q$  was considered. The additional factor being considered here is the eccentricity,  $e$ . Figure C.2 and C.3 show the influence of  $e$  on  $P_g$  and  $r$  respectively.

### C.3 Dynamic Loads

Consider the basic dynamic equation as:

$$I \ddot{\theta} + R(\theta) = M(t) \quad , \quad (C.3)$$

where

$\theta$  = rotation of soil

$$\ddot{\theta} = \frac{d^2 \theta}{dt^2} = \text{acceleration}$$

$I$  = rotational inertia

$R(\theta)$  = resistance as a function of  $\theta$

$M(t)$  = time-dependent moments.

For the failure pattern appropriate to the static loading, the terms in the dynamic equation, Eq. C.3, are:

$$I = \frac{\gamma}{g(1 + \frac{e}{r} - \frac{B}{2r})} \left[ 0.64397 r^3 + \frac{D}{3} (D^2 + r^2) + 0.78540 r \left( \frac{4r}{\pi} - D \right)^2 \right] \quad (C.4)$$

ARMOUR RESEARCH FOUNDATION OF ILLINOIS INSTITUTE OF TECHNOLOGY



$$R(\theta) = \frac{\gamma \theta}{(r + e - \frac{B}{2})} \left\{ 0.105\pi \left[ r^3 + (r + D)^3 \tan \psi \right] - \frac{D (r - B)^2}{2} \tan \lambda \right\} \quad (C.5)$$

$$M(t) = P(t) - P_g = \frac{0.106 \gamma \pi}{(r + e - \frac{B}{2})} \left[ r^3 - (r + D)^3 \right] + \frac{\gamma D (r - B)^2}{2(r + e - \frac{B}{2})} \quad (C.6)$$

where

$$\lambda = \tan^{-1} \frac{D}{r - B}$$

$\gamma$  = unit weight of soil

$$\psi = \tan^{-1} \left[ 1 - \frac{D}{0.424 (r + D)} \right]$$

$g$  = gravitational constant

$B$  = width of footing

$r$  = dimension defining location of failure surface

$D$  = depth of burial of footing

$\theta$  = rotation of soil mass about point C

$P(t)$  = time-dependent force applied to footing

$P_g$  = static capacity of footing.

The above development uses the shear surface location,  $r$ , and the load capacity,  $P_g$ , determined by the static analysis presented in the previous section. It should be emphasized, however, that the determination of the static data should be based on the best possible estimate for the soil properties; i.e., the properties should be selected to incorporate the influence of the variables involved, e.g., the rate of load application.

ARMOUR RESEARCH FOUNDATION OF ILLINOIS INSTITUTE OF TECHNOLOGY

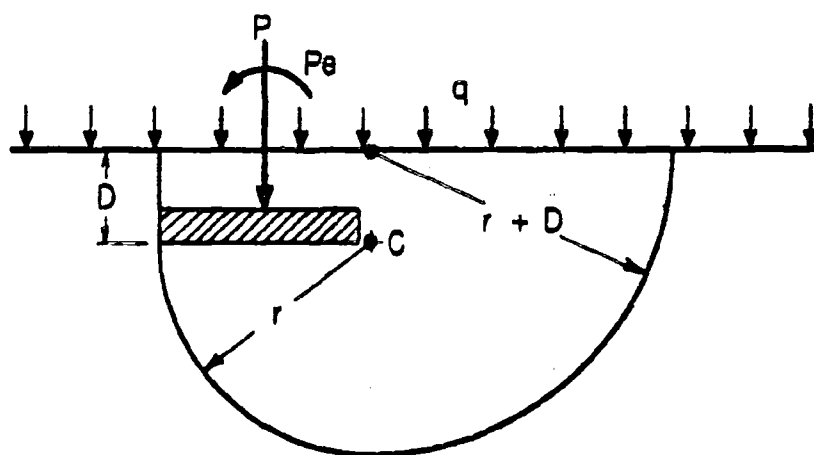


Fig. C.1. ONE-SIDED FAILURE

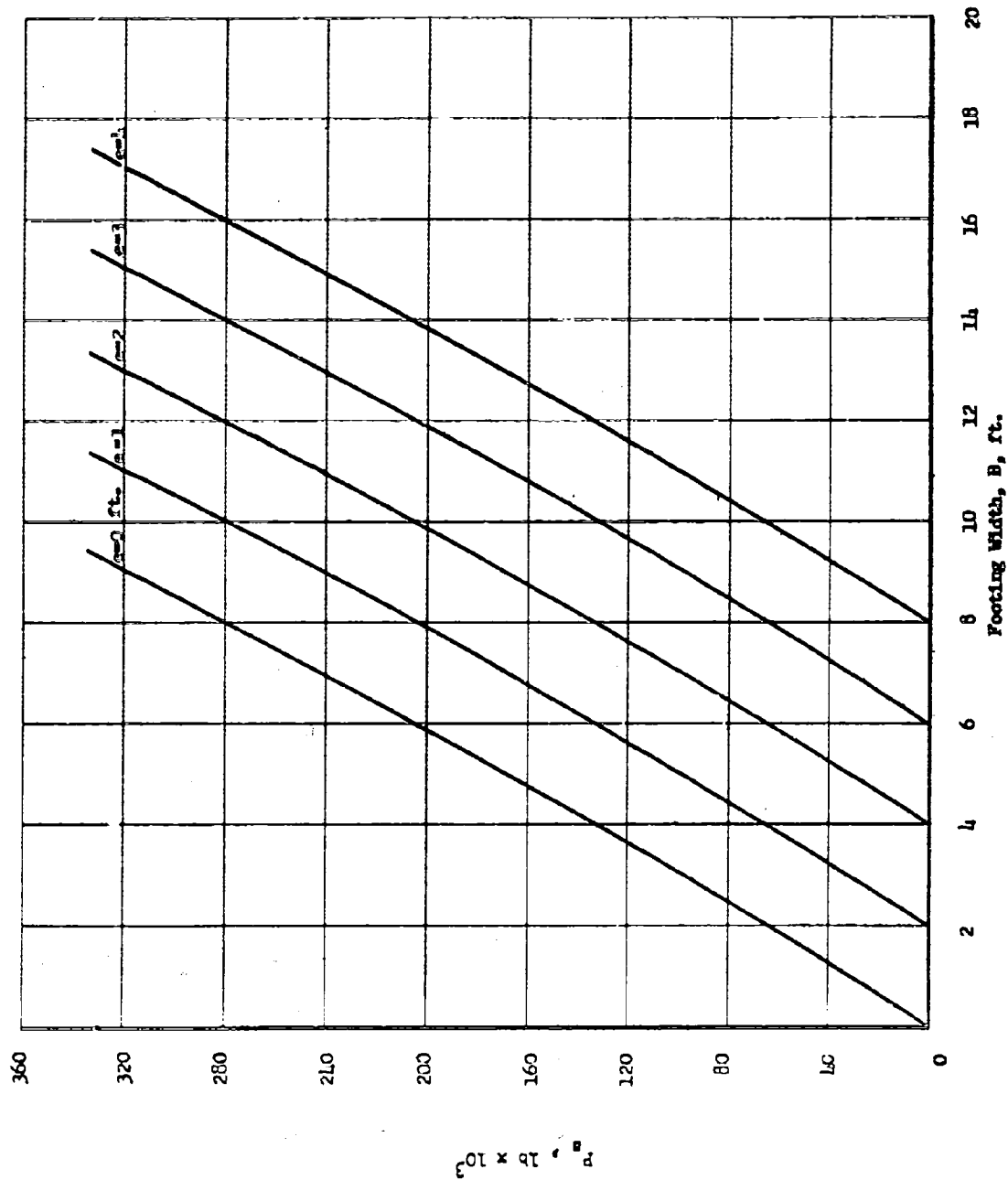


Fig. C.2 STATIC LOAD vs. FOOTING WIDTH AS A FUNCTION OF  $s$

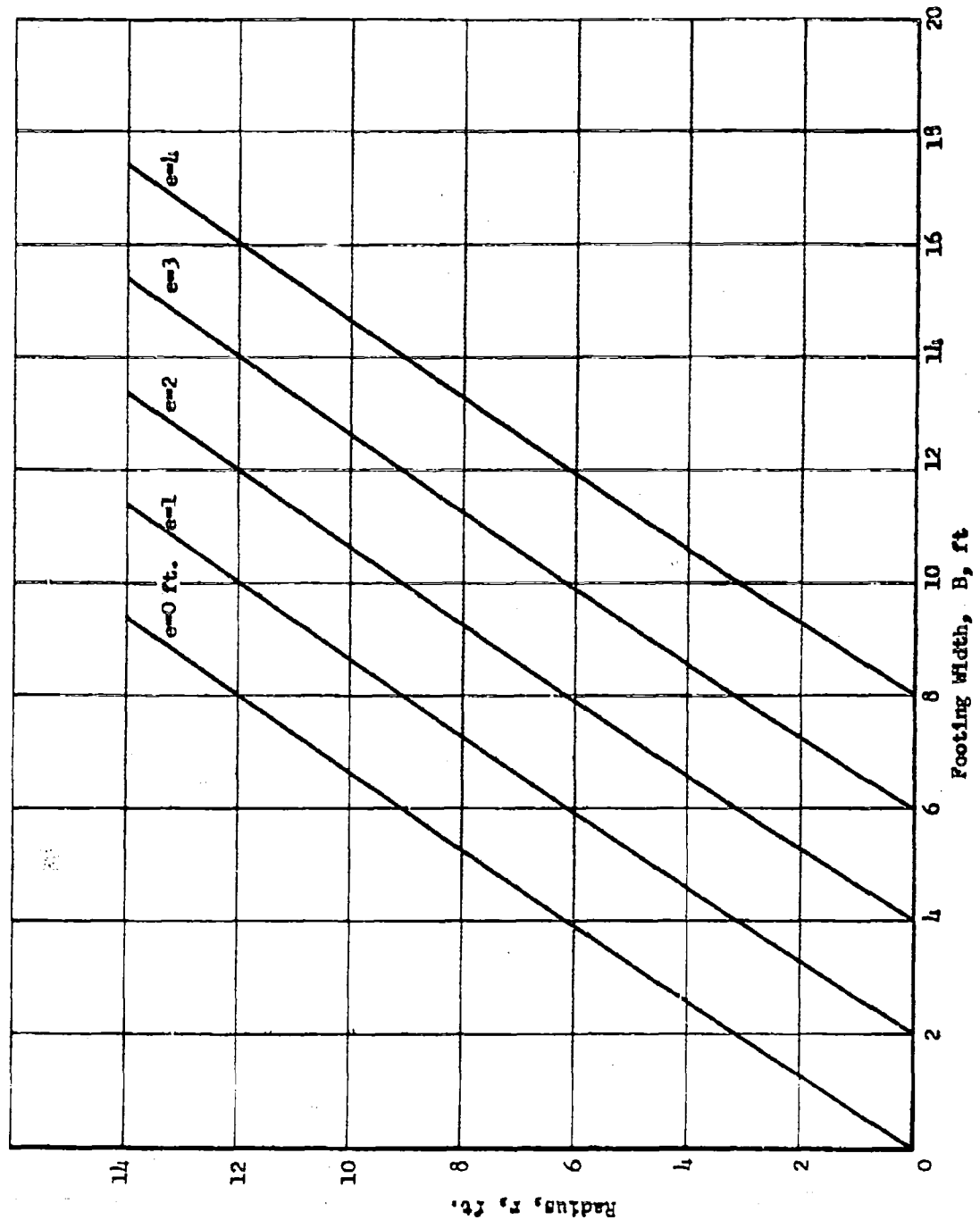


Fig. C.3 RADIUS vs. FOOTING WIDTH AS A FUNCTION OF  $e$

Appendix D

PROPERTIES OF OTTAWA SAND

ARMOUR RESEARCH FOUNDATION OF ILLINOIS INSTITUTE OF TECHNOLOGY

## Appendix D

### PROPERTIES OF OTTAWA SAND

Most of the experimental work of the original and current programs has been conducted using dry Ottawa sand. One of the puzzling aspects of the original research was the discrepancies noted between the properties of the Ottawa sand found by triaxial tests and those determined by calculations based on the footing behavior<sup>1/</sup>. This appendix contains the results of two tests which may serve to clarify this situation.

The Ottawa sand is described by the grain size distribution curve included as Fig. D.1. (The original sand is still used in the sand box, and a new sand is used in the glass box.) Figure D.2 shows the results of direct shear tests on this sand, when the density ranged from 110.0 to 117.5 pcf. (These densities are given as a range although, due to the small specimen size and other factors, they are individually not too accurate. In particular, the upper bound is higher than that previously obtained and must be questioned.) The envelopes for the maximum and minimum values of the load deflection curve are indicated.

A series of triaxial tests were conducted using specimens prepared in the Harvard Miniature Compaction Mold (1.31-in. diameter, 2.82-in. height). A number of alternate approaches for obtaining high density were investigated. It was found that densities of approximately 109 pcf could be obtained by compacting the sand in six layers using a weight of 100 gm dropped 50 times per layer from a height of 1 in. For each test, a value of the angle of internal friction  $\phi$ , was determined by passing a line through the origin tangent to the Mohr's circle. Table D.1 and Fig. D.3 show the resulting data. The curve and points on Fig. D.3 give an indication of the scatter in the data.

The experimental difficulty arises here in the determination of the density. For the mold being used, a 1-gm difference in weight represents 1 pcf. In addition, the volume of the triaxial specimen at the time of testing may differ from the volume of the mold. With respect to these factors, variations

---

<sup>1/</sup> McKee, K.E., Design and Analysis of Foundations for Protective Structures, AFSWC TR 59-56, October, 1959.

ARMOUR RESEARCH FOUNDATION OF ILLINOIS INSTITUTE OF TECHNOLOGY

of 1 pcf from the densities reported seem reasonable. In spite of these inconsistencies, the results do indicate that  $\phi$  increases substantially with density.

The results of these two test series (Fig. D.2 and D.3) establish that the angle of internal friction,  $\phi$ , for dense dry Ottawa sand can exceed  $40^\circ$  and that the exact value is a function of the density. The value of  $\phi$  found by inverse application of Terzaghi's formula<sup>2/</sup> therefore may represent an accurate value for the sand density encountered.

---

<sup>2/</sup> McKee, K. E., Op. Cit.

Table 1

RESULTS OF TRIAXIAL TESTS ON OTTAWA SAND

Density, pcf	Angle of Internal Friction, $\phi$ , deg.
102.0	26.5
105.2	31.0
105.8	33.0
107.1	34.0
107.5	33.5
107.7	35.0
107.7	33.5
107.9	33.0
108.0	37.0
108.6	32.5
109.0	41.0



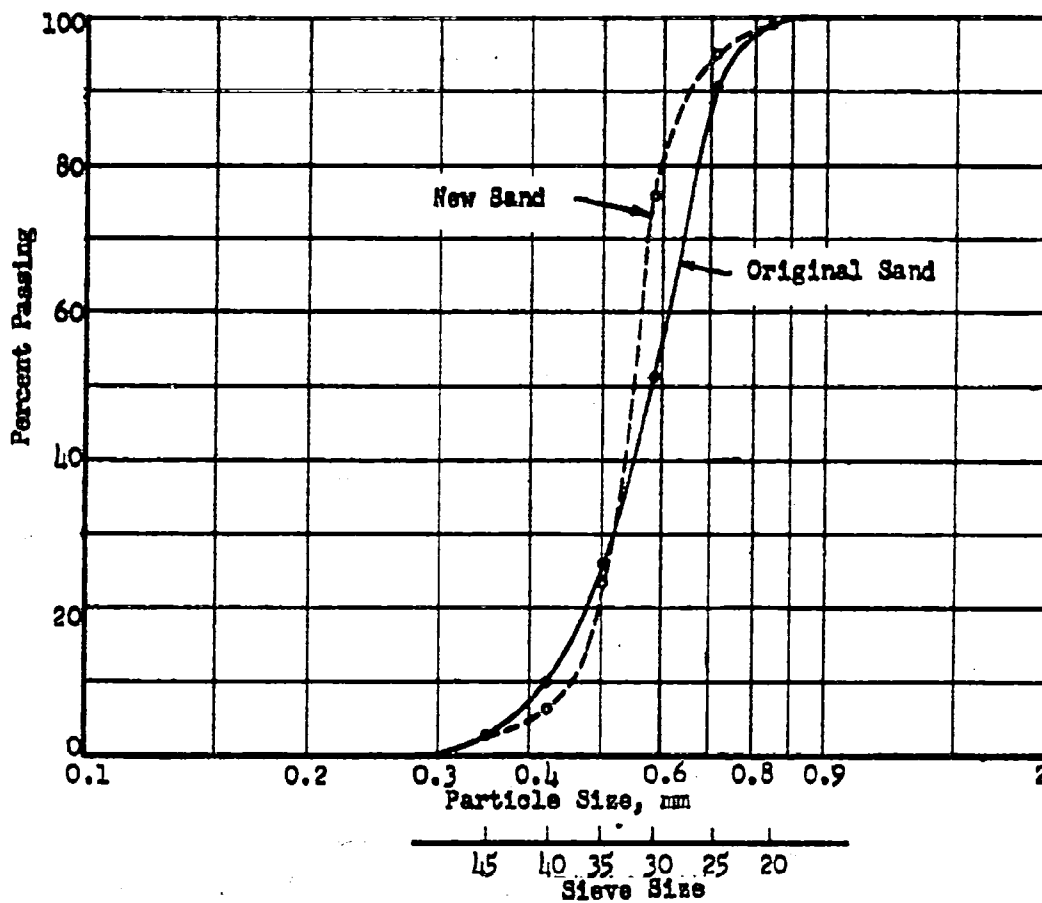


Fig. D.1 GRAIN SIZE DISTRIBUTION FOR OTTAWA SAND, BOTH  
NEW SAND AND ORIGINAL SAND

ARMOUR RESEARCH FOUNDATION OF ILLINOIS INSTITUTE OF TECHNOLOGY

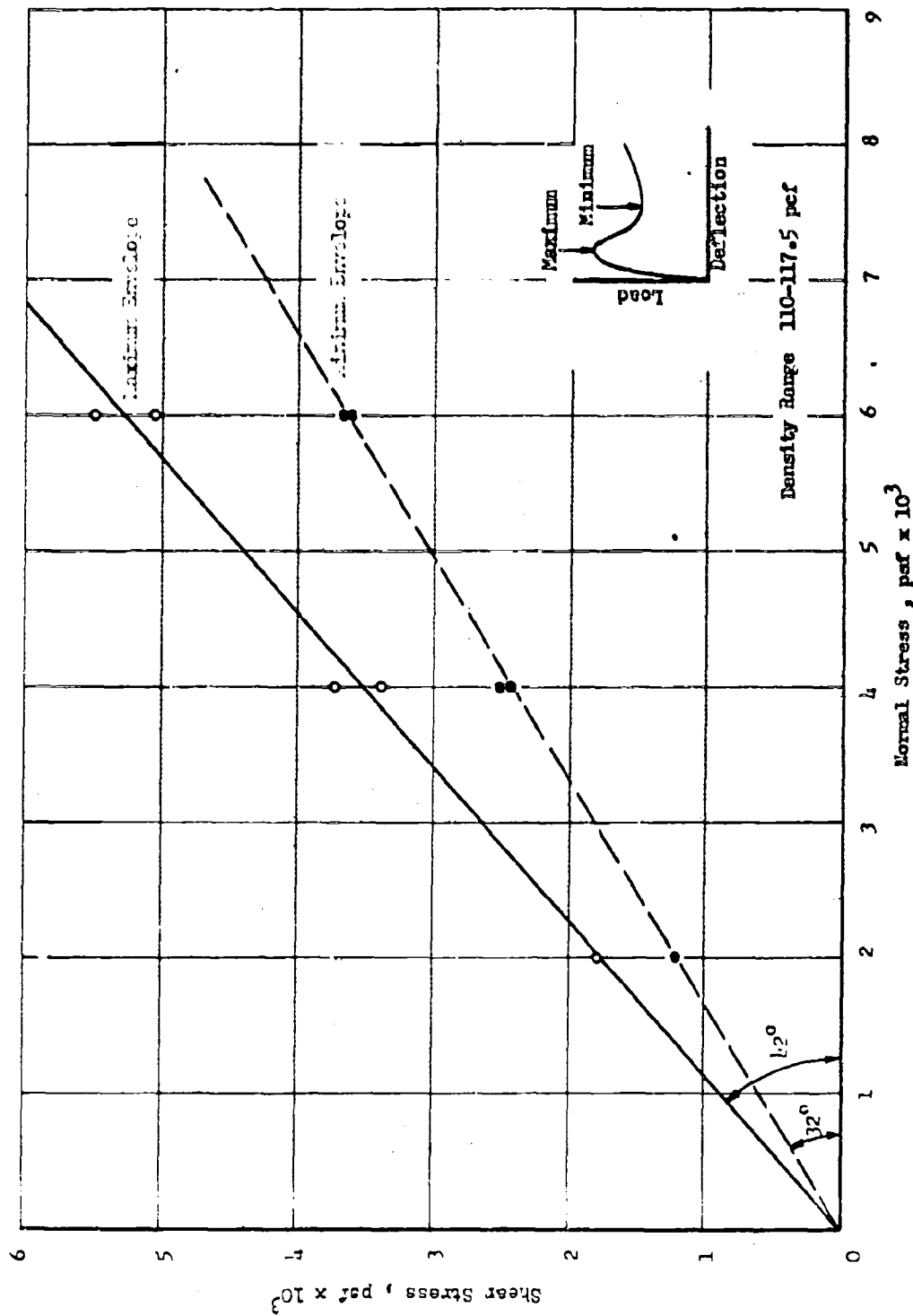


Fig. D.2 ENVELOPES FOR OTTAWA SAND AS DETERMINED FROM DIRECT SHEAR TESTS

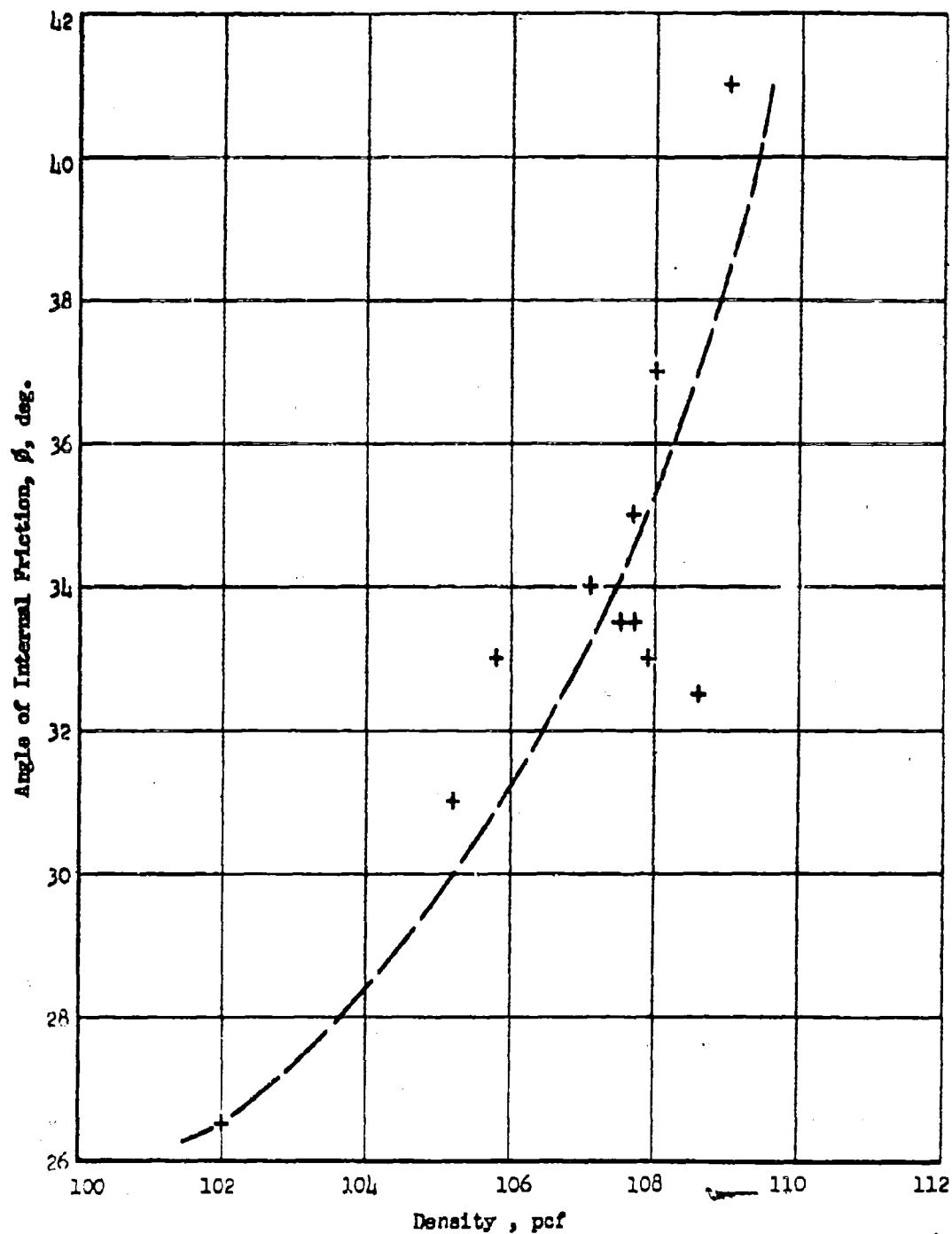


Fig. D.3 RESULTS OF TRIAXIAL TESTS ON OTTAWA SAND

ARMOUR RESEARCH FOUNDATION OF ILLINOIS INSTITUTE OF TECHNOLOGY

Appendix

TWO-DIMENSIONAL STUDIES

ARMOUR RESEARCH FOUNDATION OF ILLINOIS INSTITUTE OF TECHNOLOGY

## Appendix E

### TWO-DIMENSIONAL STUDIES

#### E.1 Introduction

Two-dimensional studies are being carried out in a glass-sided soil container. This container was designed and built during the earlier research program and is completely described in earlier reports<sup>1/</sup>. The objective of this phase of the experimental study is to obtain qualitative information regarding the influence of soil type on footings subjected to both static and dynamic loads. Because of the nature of this objective, it is essential that this phase of the experimental program be completed at the earliest possible date, since it is anticipated that the theoretical approach will be guided to a major extent by the observed results.

The range of soils considered for this phase include dense Ottawa sand, loose Ottawa sand, dense California sand, and several types of cohesive soils. The experiments considered include static and dynamic loading. For the static experiments, the procedures are following those used during the original program. For the dynamic experiments, the major observations are being made through use of Faxtax photography during the test and through before-and-after still photography. These techniques intended primarily for qualitative information are being supplemented by quantitative measurements within the limits of the experimental procedures. The limitations of this "quantitative" information should be clearly understood -- it can be meaningful or it may be satisfactory only for the purposes of comparison.

#### E.2 Static Tests

The glass box static tests to date have considered primarily dense and loose Ottawa sand; one trial run was also made with a cohesive material. These experiments were conducted with normal loading (i.e., through a hydraulic jack with the total loading occurring within 5 min.) and with mechanically controlled loading rates (i.e., the downward speed of the top of the proving ring was limited to a specified rate of 0.00053 in.

---

<sup>1/</sup> McKee, K. E., Op. Cit.

per minute). A movie camera was automatically turned on at 15- to 30-min. intervals to take 6 to 10 frames of the latter tests. Because of difficulties in reading the pages from the movie film, only limited data were obtained from the four tests. Additional experiments, where the time-lapse photograph is limited to dial pictures, will be required.

The results of the glass box tests on Ottawa sand are given on Fig. E.1 and E.2 for dense and loose sand, respectively. Tests F1 through F7 refer to normal loading rate load tests using the hydraulic jack. Tests FA through FD refer to long term experiments at controlled loading rates. In every case, the average density in the box is shown after the symbol for the test. The limited data from the experiments with controlled rate of loading shows results substantially in agreement with those for normally loaded footings. One observation from these controlled-loading rate tests is of particular interest: the load-deflection curve was not smooth. As the top of the proving ring was displaced, the load increased with essentially no increase in displacement until there was suddenly a gross motion with an associated decrease in load. This cycle was repeated throughout the duration of the loading.

With the controlled loading rate, the formation and subsequent transformation of the soil mass were observable in greater detail than previously. Figure E.3 and E.4 contain a selected series of photographs for such tests on dense and loose sand, respectively. The behavior of footings on dense sand is similar to that observed in the original program. The footings on loose sand are typified by the photographs included. Large displacements occur by local shear failure<sup>1/</sup> with indication of a shear surface appearing only at relatively large deflections (see Fig. E.4e).

### E.3 Dynamic Tests

Eight dynamic tests (six on dense Ottawa sand and two on loose Ottawa sand) have been conducted in the glass box. All of these experiments made use of the dynamic loading device constructed for this program. Instrumentation was limited to Fastax photography of the footing response. These experiments were conducted in an attempt to increase the knowledge available regarding the behavior of footings subjected to dynamic loads. It was hoped

---

<sup>1/</sup> Terzaghi, K., Theoretical Soil Mechanics, Wiley, 1943.

that this qualitative information would aid in improving the analytical techniques, while dependence was placed on the three-dimensional tests for quantitative data.

Figures E.9 and E.10 show a series of photographs taken from the fastax film for dense and loose Ottawa sand, respectively. Four of the best fastax films (two dense sand and two loose sand) were cut and spliced to form a pictorial record of the experiments. A print of this film will be made available on request to AFSC.

A single glass box test was conducted using cohesive material. The density in the box was 121.0 pcf. The loads were applied statically through a hydraulic jack. The load-displacement curve is shown on E.5, and photographs appear on Fig. E.6, E.7, and E.8. The strength of this soil was sufficient so that the glass side of the box ruptured prior to formulation of a shear surface in the soil.

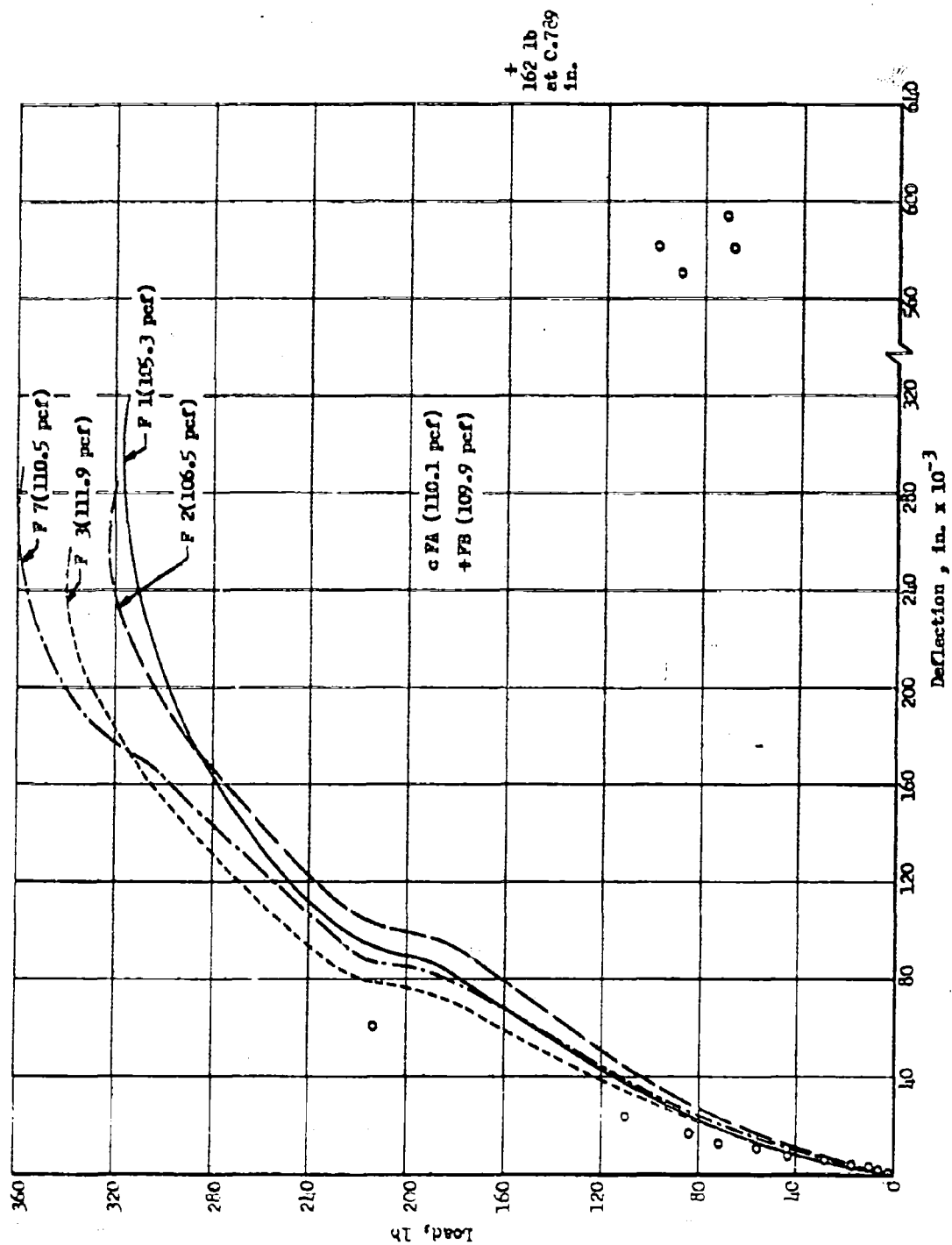


Fig. E.1 FOOTING TESTS IN GLASS BOX, DECKE SAND, 3-IN. WIDE FOOTING



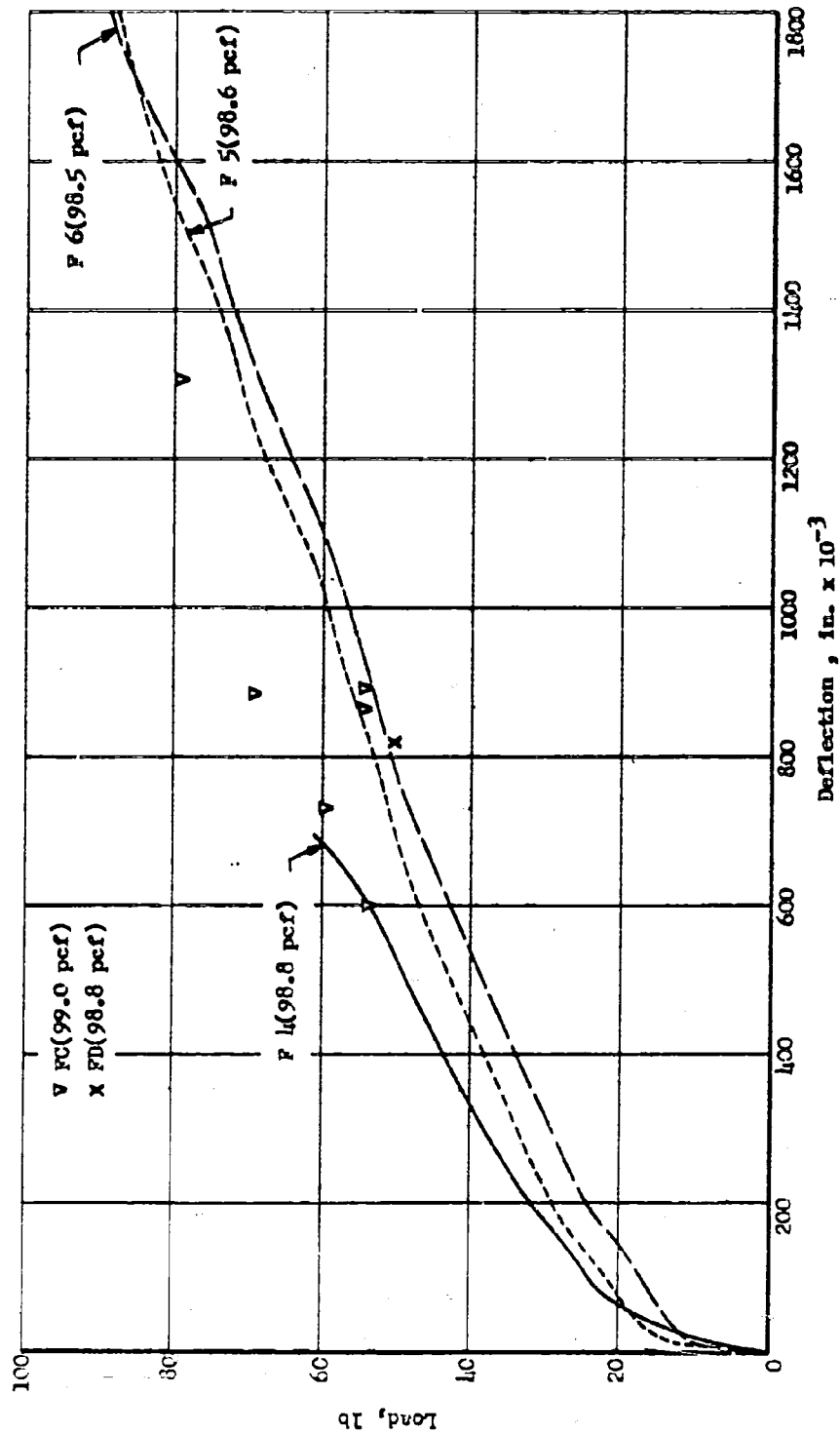
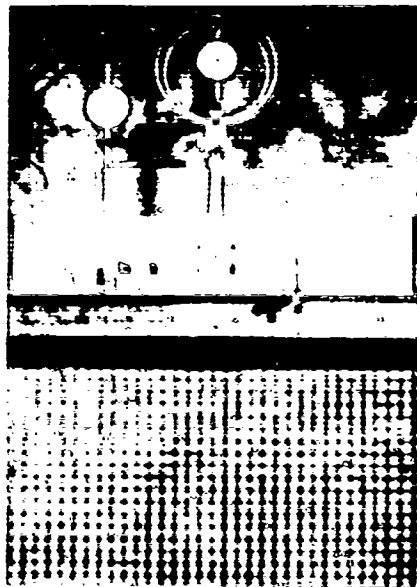


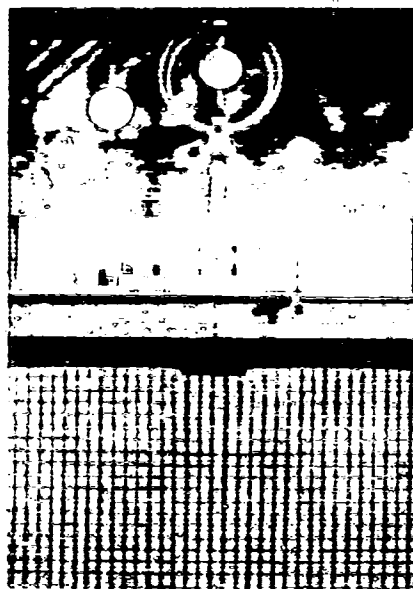
FIG. E.2 FOOTING TESTS IN GLASS BOX, LOOSE SAND, 3-IN. WIDE FOOTING



(a)



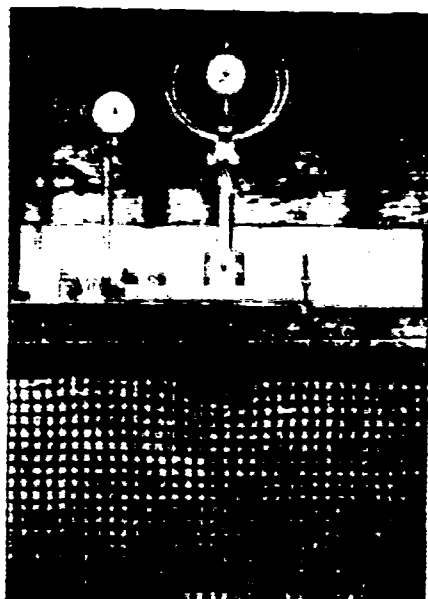
(b)



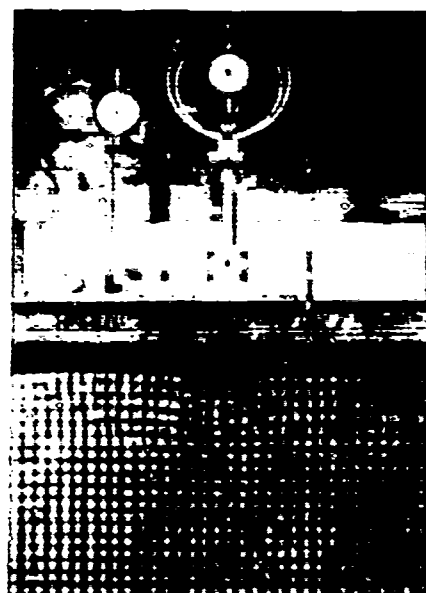
(c)

Fig. E.3 STATIC FOOTING FAILURE ON DENSE SAND

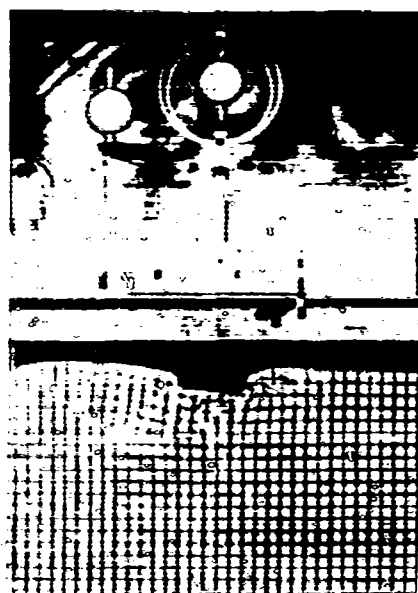
ARMOUR RESEARCH FOUNDATION OF ILLINOIS INSTITUTE OF TECHNOLOGY



(d)



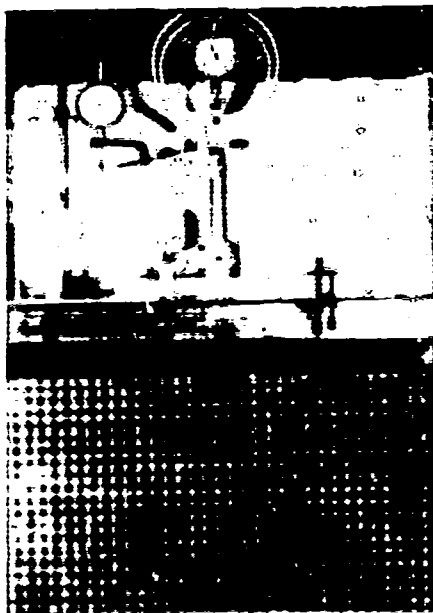
(e)



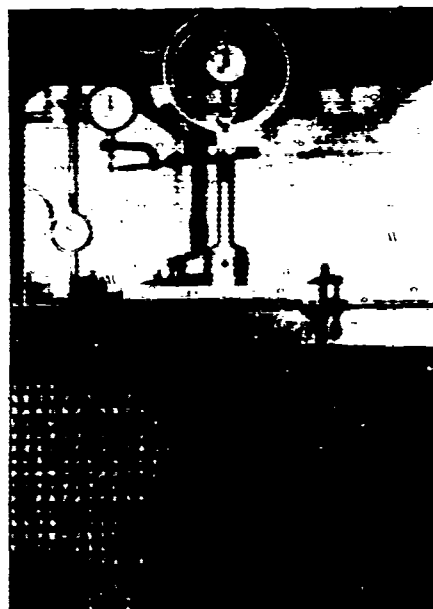
(f)

Fig. E.3 STATIC FOOTING FAILURE ON DENSE SAND (cont)

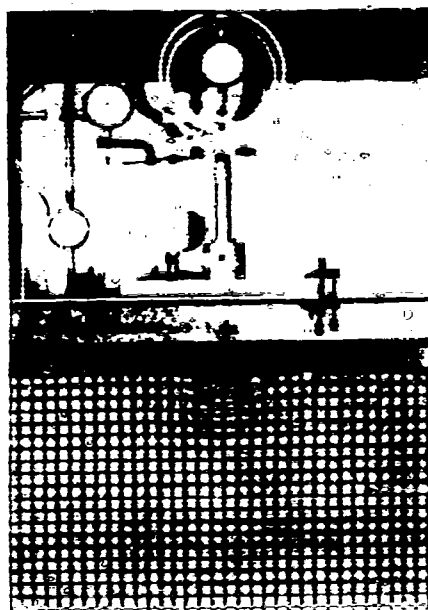
ARMOUR RESEARCH FOUNDATION OF ILLINOIS INSTITUTE OF TECHNOLOGY



(a)



(b)



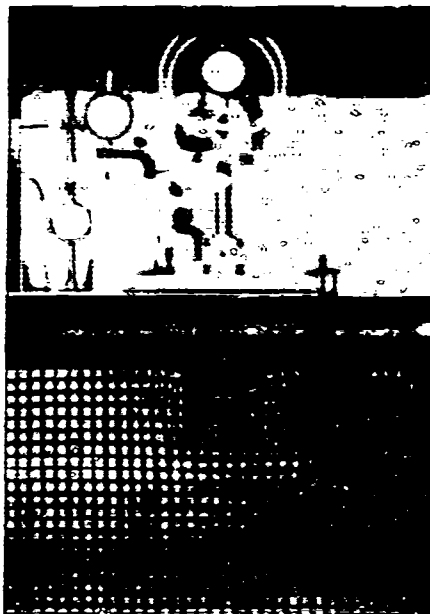
(c)

Fig. E.4 STATIC FOOTING FAILURE ON LOOSE SAND

ARMOUR RESEARCH FOUNDATION OF ILLINOIS INSTITUTE OF TECHNOLOGY



(d)



(e)

Fig. E.4 STATIC FOOTING FAILURE ON LOOSE SAND (cont)

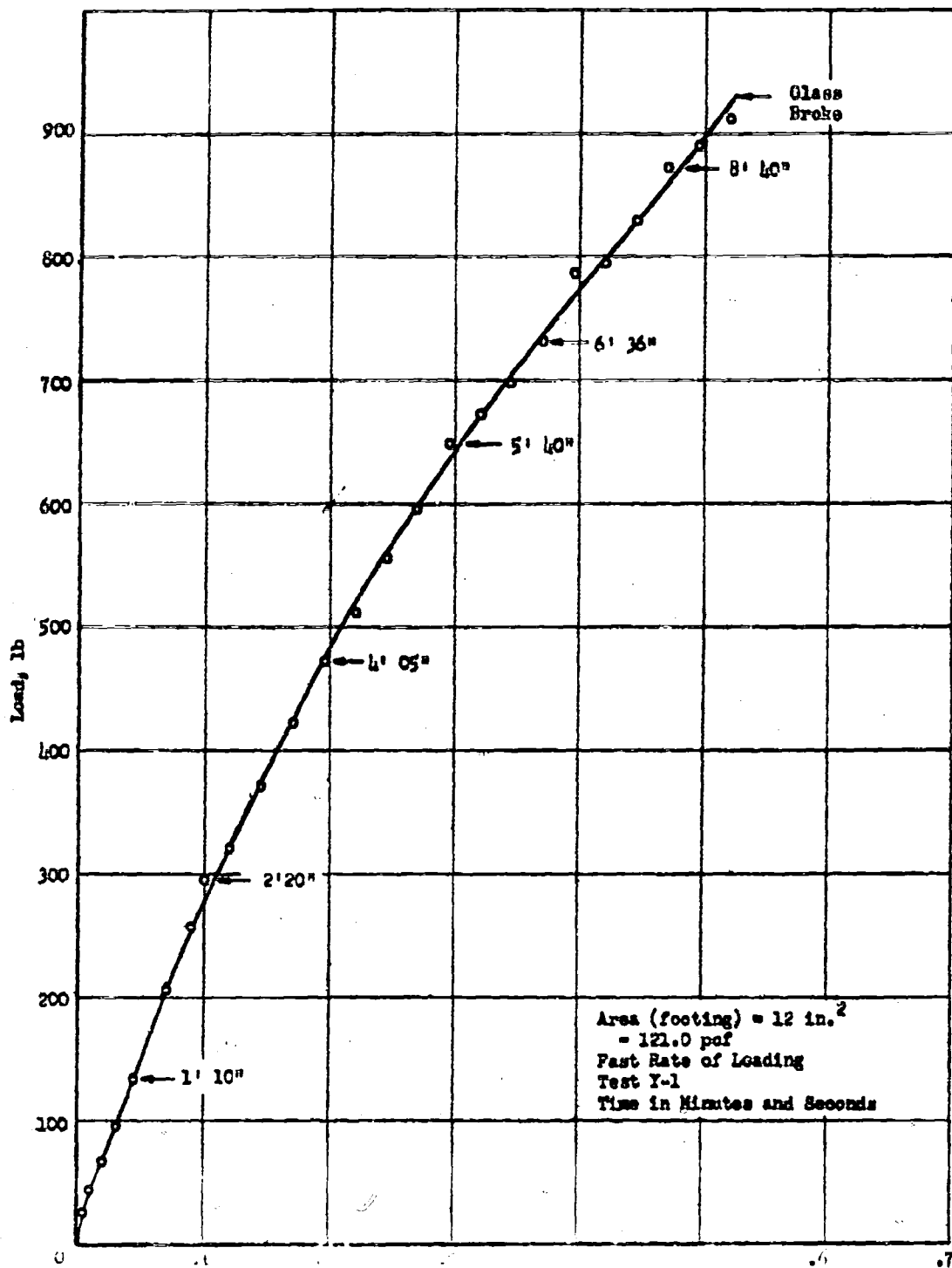


Fig. E.5 FOOTING BEHAVIOR ON COHESIVE SOIL

ARMOUR RESEARCH FOUNDATION OF ILLINOIS INSTITUTE OF TECHNOLOGY

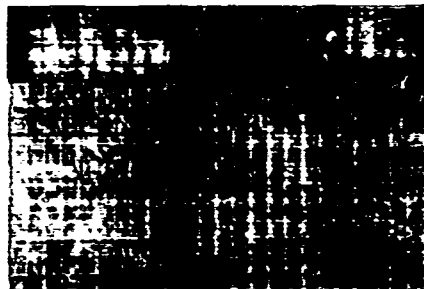


Fig. E.6 COHESIVE SOIL IN GLASS BOX BEFORE TEST

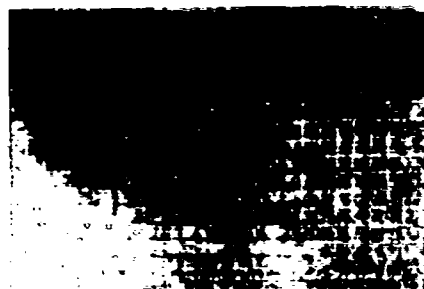


Fig. E.7 COHESIVE SOIL IN GLASS BOX DURING TEST

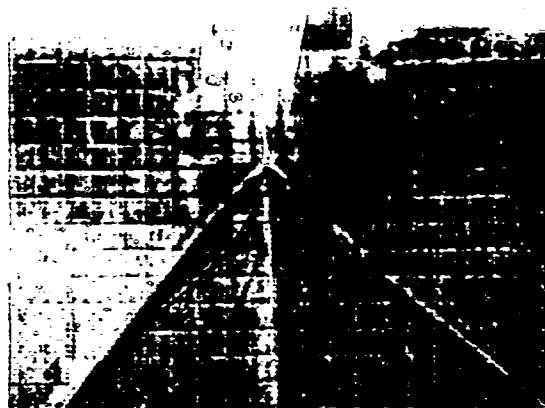
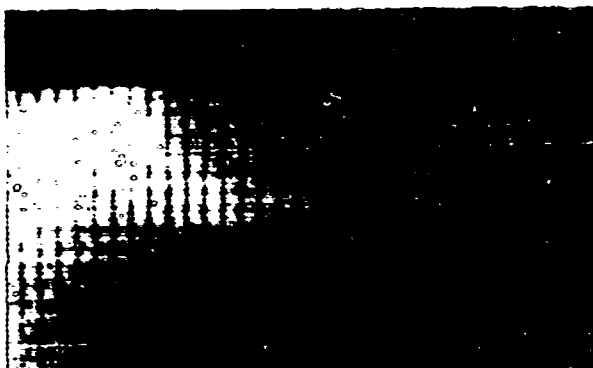
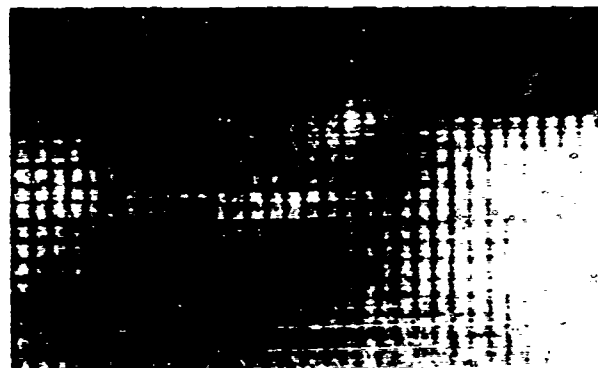


Fig. E.8 COHESIVE SOIL AFTER GLASS IN BOX FAILED



Start of Test



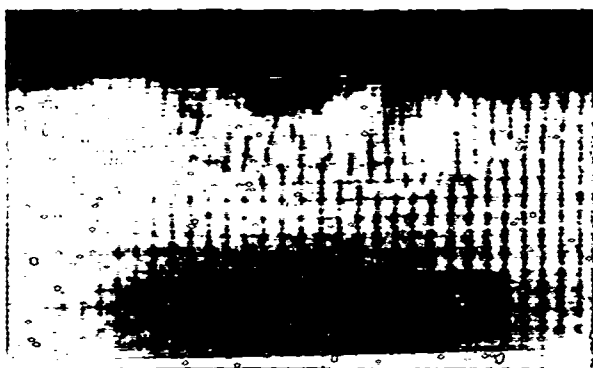
25 msec



39 msec



43 msec



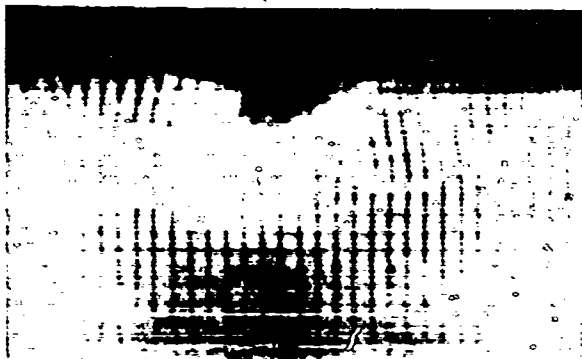
48 msec



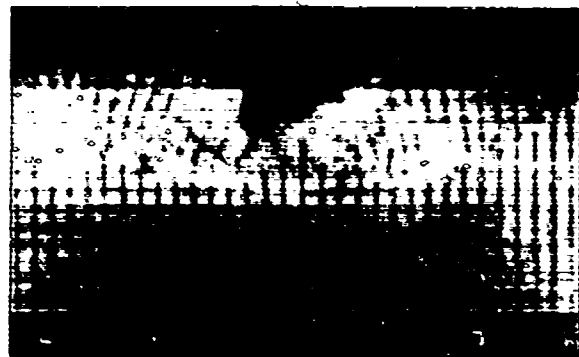
52 msec

Fig. E.9 DYNAMIC TEST OF FOOTING ON DENSE OTTAWA SAND





62 msec



74 msec



106 msec



168 msec

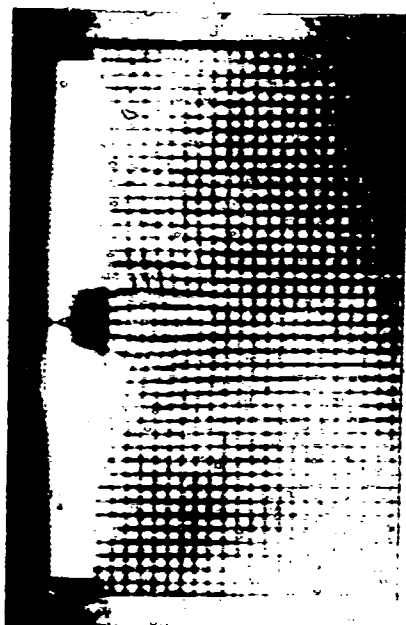


End of Test

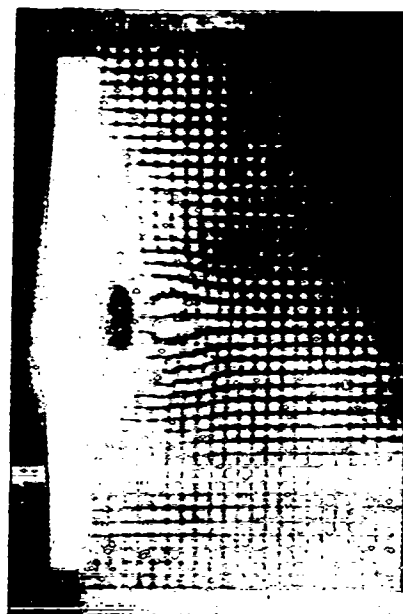
Fig. E.9 DYNAMIC TEST OF FOOTING ON DENSE OTTAWA SAND (cont)



Start of Test



50 ms



87 ms



End of Test

Fig. E.10 DYNAMIC TEST OF FOOTING ON LOOSE OTTAWA SAND

Appendix F

THREE-DIMENSIONAL STUDIES

## Appendix F

### THREE-DIMENSIONAL STUDIES

#### F.1 Introduction

Three-dimensional studies are being carried out in the sand box used during the earlier research on this project. This box is 4-ft square in plan and 3-ft deep. The objective of this phase of the experimental study is to obtain quantitative information on the behavior of footings subjected to static and dynamic loads. During the original project, static loads and dropped weights were applied to footings placed on dense dry Ottawa sand.

The soils to be considered in the sand box tests are being limited to dense Ottawa and dense California sand. Within the scope of the present program, consideration of cohesive materials is thought not to be practical, as the control required in laboratory experiments, the mixing and placing of cohesive materials offers extreme difficulty; even for very small specimens, the maintenance of uniformity of density and ingredients requires rather extreme precautions. Certainly the size of the three-dimensional container, i.e., 4 ft x 4 ft x 3 ft, precludes its use for cohesive materials without elaborate mixing and placing apparatus. If in the future experiments using cohesive materials are planned, it is strongly recommended that consideration be given to using the smallest soil specimen size consistent with the required results.

The three-dimensional experiments were intended primarily to yield quantitative data. For this reason, emphasis has been placed on selecting the proper gages, recording systems, etc. Visual observations and photographic records have been made, but only for general coverage of the experiments.

#### F.2 Static Tests

As part of the original program, a series of footings on dense dry Ottawa sand were subjected to static loads. The results of these tests were included in Appendix A of the Final Report<sup>1/</sup>. Additional static experi-

<sup>1/</sup> McKee, K. E., Design and Analysis of Foundations for Protective Structures, AFSWC TR 59-56, October, 1959.  
ARMOUR RESEARCH FOUNDATION OF ILLINOIS INSTITUTE OF TECHNOLOGY

ments on Ottawa sand were not required and hence no static experiments have been conducted to date.

Static tests will be conducted with California sand (shipped from Naval Civil Engineering Laboratory for use in this study). The aim of these planned experiments will be to obtain sufficient data to compare the results with those for Ottawa sand. It is anticipated that this correlation can be achieved by use of the failure theories for footings. If this proves correct, only a limited number of experiments will be required.

Three-dimensional static experiments using loose sand, either Ottawa or California, could be conducted. Placement of the sand in a loose state would require a major effort for each experiment. The advantage of three-dimensional experiments using loose sand will be weighed against the complexity of conducting such experiments.

### F.3 Dynamic Tests

The dynamic loading apparatus is described in Appendix G. Much of the developmental experimentation for this device was conducted with footings placed on the surface of the sand box. Although meaningful records were obtained during many of these preliminary experiments, it was decided to make use only of records obtained using the final apparatus. These records are in the form of oscillograms. The data are a force-time record from the force washer and a displacement-time record from the LVDT (Linear Variable Differential Transformer). Visual observations are made before and after each loading. To date, only limited results are available and no attempt has been made to analyze the records obtained. Examples of these records are given in Appendix G. Figures F.1 and F.2 show examples of footing failure under dynamic loads. All of the dynamic experiments have been conducted using dense Ottawa sand. More detailed coverage of these dynamic results will be presented in the final report on the current project.



Fig. F.1 4-in. SQUARE FOOTING AFTER FAILURE



Fig. F.2 3-in. SQUARE FOOTING AFTER FAILURE

Appendix G

DYNAMIC LOADING APPARATUS

ARMOUR RESEARCH FOUNDATION OF ILLINOIS INSTITUTE OF TECHNOLOGY

ARF Project No. 8193-7  
Interim Report

Appendix G  
DYNAMIC LOADING APPARATUS

An apparatus suitable for applying dynamic loads to small footings has been developed. This apparatus is designed to provide controlled loadings with minimum complexity. "Controlled" refers to the ability to determine the loads that are applied. Variations in the parameter defining the loads are introduced, but no stringent requirements are enforced on these variations as long as the resulting force-time history can be measured. The final design of the apparatus is the result of modifications introduced during preliminary testing to achieve the desired end result. Thus, little could be gained by discussing the design development, and attention will be confined to describing the present laboratory setup. As of this writing, the research using the dynamic loading device is preliminary in nature with the main objective being equipment development, calibration, etc. In the course of this work, however, footings have been tested, loads measured, etc., thus providing some quantitative data.

Figure G.1 shows a sketch of the experimental setup. Figures G.2 and G.3 show the dynamic loading apparatus attached to the glass box and sand box respectively. The operation of the dynamic device is relatively simple. With the solenoid-operated valve closed, pressure is released from the nitrogen bottle into the air accumulator and hydraulic accumulator, so that pressure builds up in the hydraulic fluid behind the valve. To apply a dynamic load the valve is opened, allowing hydraulic pressure to be applied to the piston. The load transmitted to the footing is measured by a force washer<sup>1</sup>. The equipment described herein produced rise times of from 2 to 5ms in the loads acting on the footings. The displacement of the footing is measured by a linear variable transducer -- the assumption being that this measurement represents the displacement of the center of the footing.

The experimental studies with the dynamic apparatus have been preliminary in nature. An attempt is always made to obtain a reasonable amount of data, but primary emphasis to date has been on checking out the equipment. The preliminary tests were conducted, with the displacements and loads being

---

<sup>1</sup> Lockheed Electronics Model WR7S High Sensitivity Force Washer.



recorded by a Polaroid photograph of the oscilloscope screen. Although these records were sufficient for this preliminary work, a Consolidated recorder has been introduced for experiments where the data are of prime importance. The following paragraphs present a general description of the operation of the dynamic apparatus.

Figures G.4 and G.5 show two examples of the records obtained from the oscilloscope. Figure G.4 shows a more-or-less linearly decaying force with a relatively small maximum displacement, approximately 0.1 in. Figure G.5 shows a larger displacement, approximately 1.0 in., and a force that drops off after about 100 ms.

Figure G.6 and G.7 are examples of records obtained by the Consolidated recorder. These records read from right to left. Both displacement records are beyond the linear range of the recorder -- this explains the apparent recovery after the initial peak. The records are meaningful up to the maximum displacement, but beyond that point it is only possible to deduce that the footings stopped moving. Figures G.6 and G.7 show respectively a relatively long and a relatively short duration of load application.

The advantage of the records obtained from the Consolidated recorder for quantitative data is obvious. For this reason, it is anticipated that this method will be used for the remainder of the dynamic experiments. By varying the initial pressure, the status of needle valve, etc., it is possible to vary both the shape and magnitude of the load obtained from the system. Current work is still concerned with learning to control these parameters.

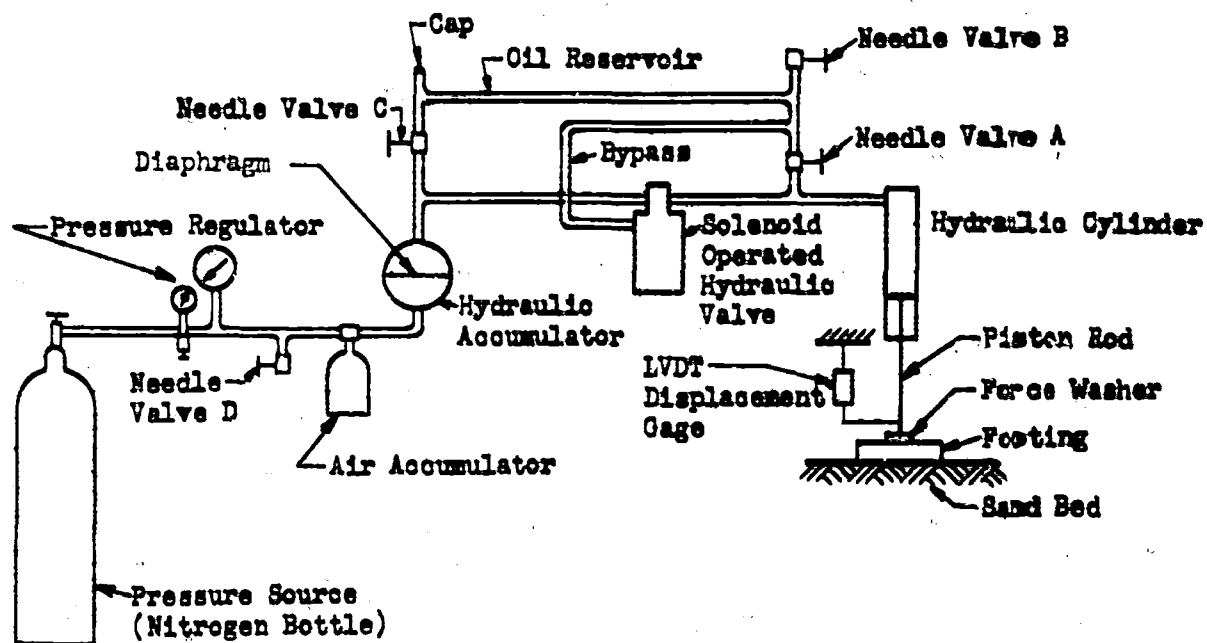


Fig. G.1 SKETCH OF DYNAMIC APPARATUS

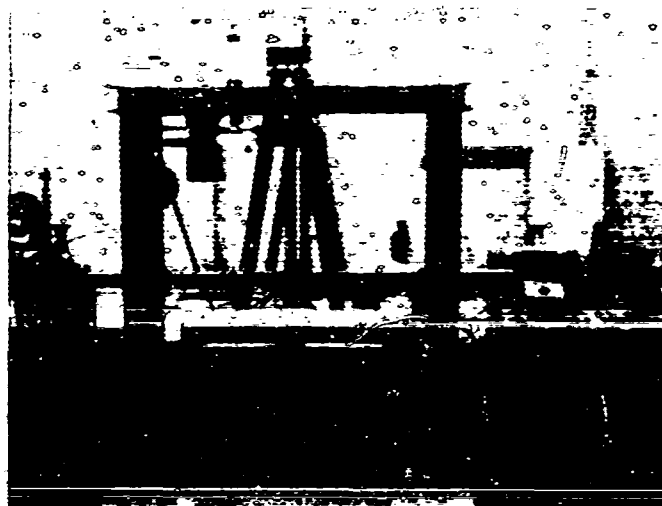


Fig. G.2 DYNAMIC APPARATUS ON GLASS BOX

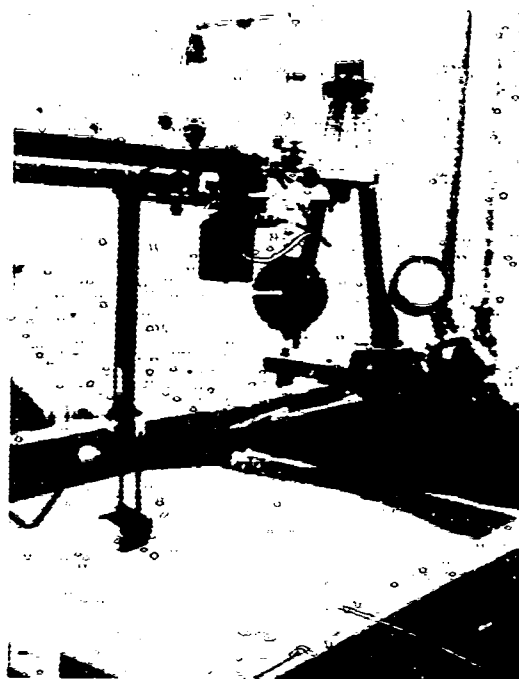
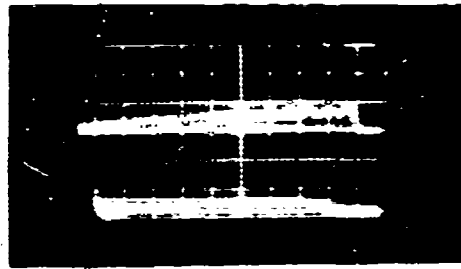
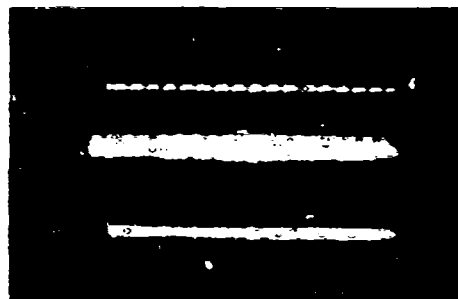


Fig. G.3 DYNAMIC APPARATUS ON SAND BOX



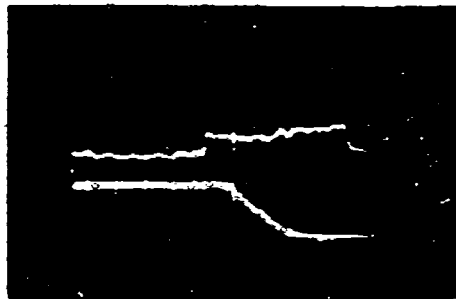
(a) Record



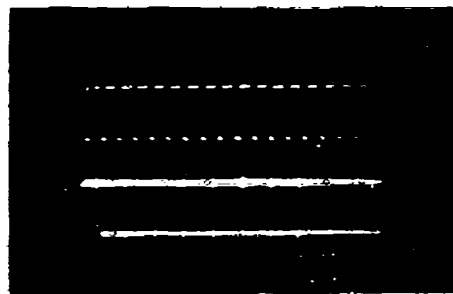
(b) Calibration

Fig. G.4 RECORDS FOR 4-in.x-4-in. FOOTING, TEST NO.6

Records read right to left. Top trace is force;  
Bottom trace is displacement.



(a) Record



(b) Calibration

Fig. G.5 RECORDS FOR 4-in.x-4-in. FOOTING, TEST NO. 2

Records read right to left. Top trace is force;  
Bottom trace is displacement.

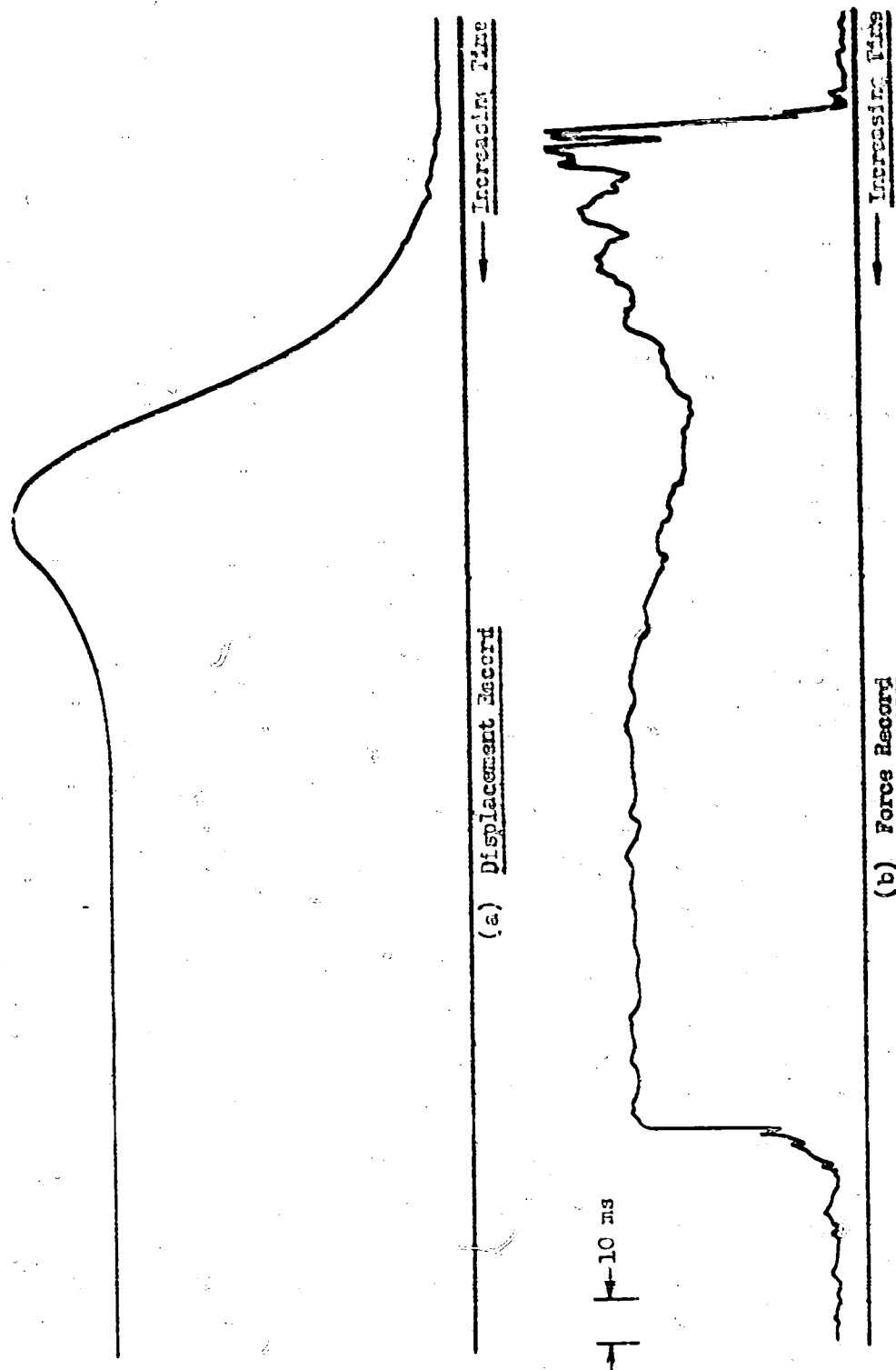


Fig. 0.6 TYPICAL CONSOLIDATED RECORDS, TEST NO. 1

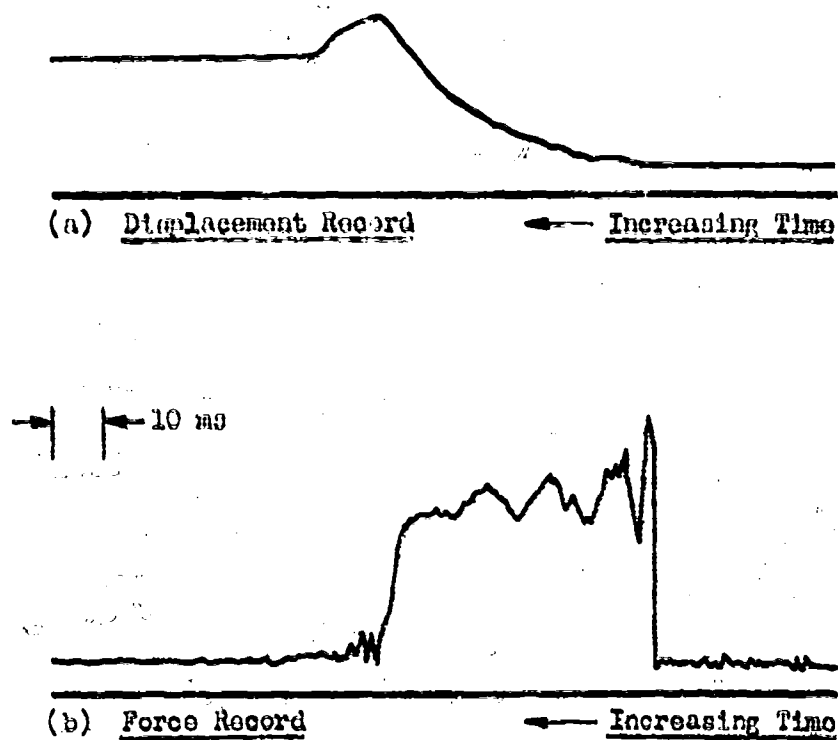


Fig. G.7 TYPICAL CONSOLIDATED RECORDS, TEST NO. 10

## DISTRIBUTION

No. Cys

1	Hq USAF (AFDRT), Wash 25, DC
1	Hq USAF (AFCIN-3B), Wash 25, DC
1	USAF Dep IG for Insp (AFCDI-B-3), Norton AFB, Calif
1	USAF Dep IG for Safety (AFCNS), Kirtland AFB, NMex
1	AFBMD (WDFN), AF Mail Post Office, Los Angeles 45, Calif
1	AUL, Maxwell AFB, Ala
	WADD, Wright-Patterson AFB, Ohio
1	(Director of Sys Mgt)
1	(WWAD)
	AFSWC, Kirtland AFB, NMex
1	(SWNI)
15	(SWOI)
3	(SWRS)
1	Director, US Army Waterways Experiment Station, ATTN: WESRI, P. O. Box 60, Vicksburg, Miss
2	Chief of Engineers, Department of the Army, ATTN: ENGEB, Wash 25, DC
1	Commanding Officer and Director, Naval Civil Engineering Laboratory, Port Huene, Calif
1	Chief, Defense Atomic Support Agency, ATTN: Blast and Shock Branch, Wash 25, DC
10	ASTIA (TIPDR), Arlington Hall Sta, Arlington 12, Va
1	University of Illinois, ATTN: Dr. Nathan M. Newmark, Head, Department of Civil Engineering, 207 Talbot Laboratory, Urbana, Ill
5	Armour Research Foundation, Illinois Institute of Technology, 3422 South Dearborn St., Chicago 16, Ill
1	Massachusetts Institute of Technology, Dept of Civil and Sanitary Engineering, ATTN: Dr. Whitman, 77 Massachusetts Avenue, Cambridge 39, Mass
1	University of Illinois, ATTN: Dr. H. O. Ireland, 207 Talbot Laboratory, Urbana, Ill